Three-dimensional seismic velocity structure and configuration of the Philippine Sea slab in southwestern Japan estimated by double-difference tomography

doi: 10.1029/2007JB005274

Three-dimensional seismic velocity structure and configuration of the Philippine Sea slab in southwestern Japan estimated by double-difference tomography

Fuyuki Hirose,[1] Junichi Nakajima,[2] and Akira Hasegawa[2]

Received 18 July 2007; revised 23 June 2008; accepted 17 July 2008; published 26 September 2008.

[1] Three-dimensional seismic velocity structure in and around the Philippine Sea plate subducting beneath southwestern (SW) Japan is determined by applying double-difference tomography method to arrival time data for earthquakes obtained by a dense nationwide seismic network in Japan. A region of low S wave velocity and high Vp/Vs of several kilometers in thickness is recognized immediately above the region of intraslab seismicity in a wide area from Tokai to Kyushu. This characteristic layer dips shallowly in the direction of slab subduction. Compared with the upper surface of the Philippine Sea slab based on seismic reflection and refraction surveys on seven survey lines, we interpret that the low-Vs and high-Vp/Vs layer corresponds to the oceanic crust of the Philippine Sea slab. On the basis of the position of the low-Vs and high-Vp/Vs layer and the precisely relocated hypocenter distribution of intraslab earthquakes, the upper surface of the Philippine Sea slab is reliably determined for the entire area of SW Japan. Nonvolcanic deep low-frequency earthquakes that occurred associated with the subduction of the Philippine Sea slab are distributed along the isodepth contour of 30 km in SW Japan, except for the Tokai district where the depth of deep low-frequency earthquakes becomes gradually deeper toward northeast.

Citation: Hirose, F., J. Nakajima, and A. Hasegawa (2008), Three-dimensional seismic velocity structure and configuration of the Philippine Sea slab in southwestern Japan estimated by double-difference tomography, *J. Geophys. Res.*, *113*, B09315, doi:10.1029/2007JB005274.

1. Introduction

[2] In southwestern Japan, the Philippine Sea plate is subducting beneath the land area in the west-northwest direction at a rate of 2–6 cm/a [*Seno et al.*, 1993; *Wei and Seno*, 1998; *Heki and Miyazaki*, 2001; *Miyazaki and Heki*, 2001]. Many phenomena with different time constants occur associated with the subduction of this young Philippine Sea plate, including long-term slow slip events in the Tokai region and the Bungo Channel [*Hirose et al.*, 1999; *Ozawa et al.*, 2001, 2002; *Miyazaki et al.*, 2006], short-term slow slip events from the Tokai region to western Shikoku [*Obara et al.*, 2004], nonvolcanic deep tremors and low-frequency earthquakes [*Obara*, 2002], and very low frequency earthquakes [*Ito et al.*, 2007]. Along the Nankai Trough, many large earthquakes have occurred in the past (Earthquake Research Committee, Long-term evaluation of earthquakes in the Nankai trough, 2001, available at http://www.jishin.go.jp/main/chousa/01jun_kitakami/index.htm), and there is concern that such large events will be repeated in the present century. However, the structure of the Philippine Sea plate, which is one of the principal causes of these events, remains poorly understood. As the plate exhibits relatively low seismic activity, with an almost complete absence of interplate earthquakes, the boundary between the continental plate and the Philippine Sea plate has proven difficult to determine reliably.

[3] In previous research on seismic activity related to the Philippine Sea slab [e.g., *Ishida*, 1992; *Noguchi*, 1996; *Miyoshi and Ishibashi*, 2004], the upper envelope of intraslab earthquakes has been regarded as the plate boundary. The configuration of the Philippine Sea slab for the entire region of SW Japan recently proposed by *Nakajima and Hasegawa* [2007] is also referred to the upper envelope of intraslab earthquakes to delineate the plate boundary for the seismic portion of the slab. However, from the Tokai region to southern Kyushu, interplate earthquakes are extremely rare, and simply regarding the upper limit of intraslab earthquakes as the plate boundary is considered an unreliable approach. In recent years, seismic wide-angle reflection and refraction surveys spanning from the Pacific ocean to the Japanese Islands have been carried out in regions including Tokai, Kinki, and Shikoku, and have suggested that the plate boundary is located several kilometers shallower than the upper limit of intraslab seismicity [*Kodaira et al.*, 2000, 2002; *Kurashimo et al.*, 2002; *Kodaira et al.*, 2004; *Ito et al.*, 2005]. This implies that there is a high

[1] Seismology and Volcanology Research Department, Meteorological Research Institute, Tsukuba, Japan.
[2] Research Center for Prediction of Earthquakes and Volcanic Eruptions, Graduate School of Science, Tohoku University, Sendai, Japan.

0148-0227/08/2007JB005274$09.00

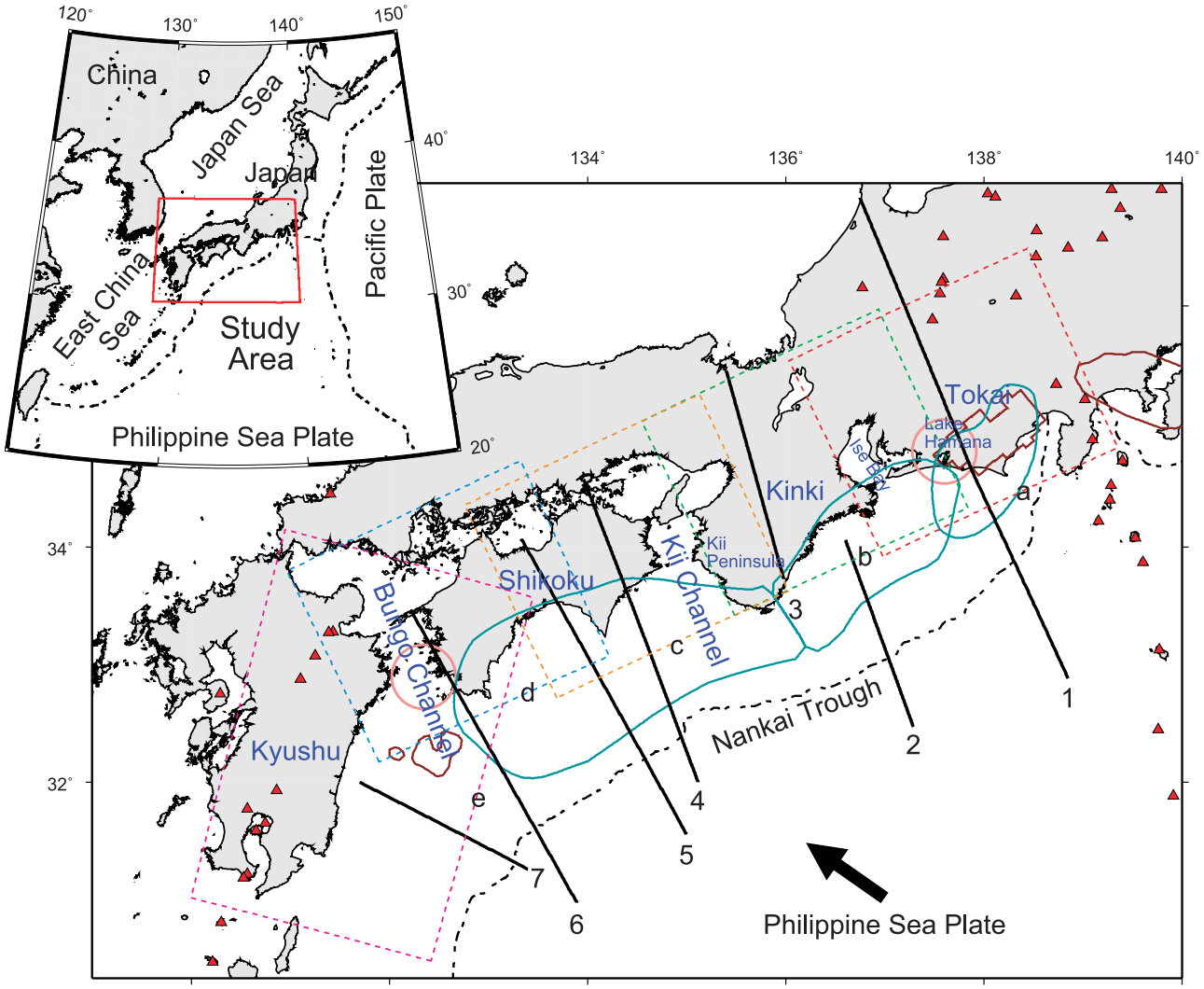

Figure 1. Map of southwestern Japan. Colored rectangles a through e denote study areas. Red triangles denote active volcanoes. Pink circles denote the long-term slow slip events beneath Lake Hamana and the Bungo Channel [*Hirose et al.*, 1999; *Ozawa et al.*, 2001, 2002; *Miyazaki et al.*, 2006]. Seismic reflection and refraction survey lines (1, *Kodaira et al.* [2004]; 2, *Nakanishi et al.* [2002]; 3, *Ito et al.* [2005]; 4, *Kodaira et al.* [2002]; 5, *Kodaira et al.* [2000]; 6, *Takahashi et al.* [2002]; 7, *Ichikawa et al.* [1997]) are indicated by black lines. Areas enclosed by blue lines represent the expected source region of the Tokai earthquake (Central Disaster Management Council, Report of the specialized investigation committee about Tokai earthquake, 2001, available at http://www.bousai.go.jp/jishin/chubou/20011218/siryou2-2.pdf), the Tonankai earthquake, and the Nankai earthquake (Earthquake Research Committee, Long-term evaluation of earthquakes in the Nankai trough, 2001, available at http://www.jishin.go.jp/main/chousa/01jun_kitakami/index.htm). Areas enclosed by brown lines denote the estimated asperities or locked zone on the Philippine Sea slab [*Wald and Somerville*, 1995; *Matsumura*, 1997; *Yagi et al.*, 1998]. Arrow indicates direction of plate motion of the Philippine Sea plate relative to the continental plate [*Wei and Seno*, 1998; *Heki and Miyazaki*, 2001].

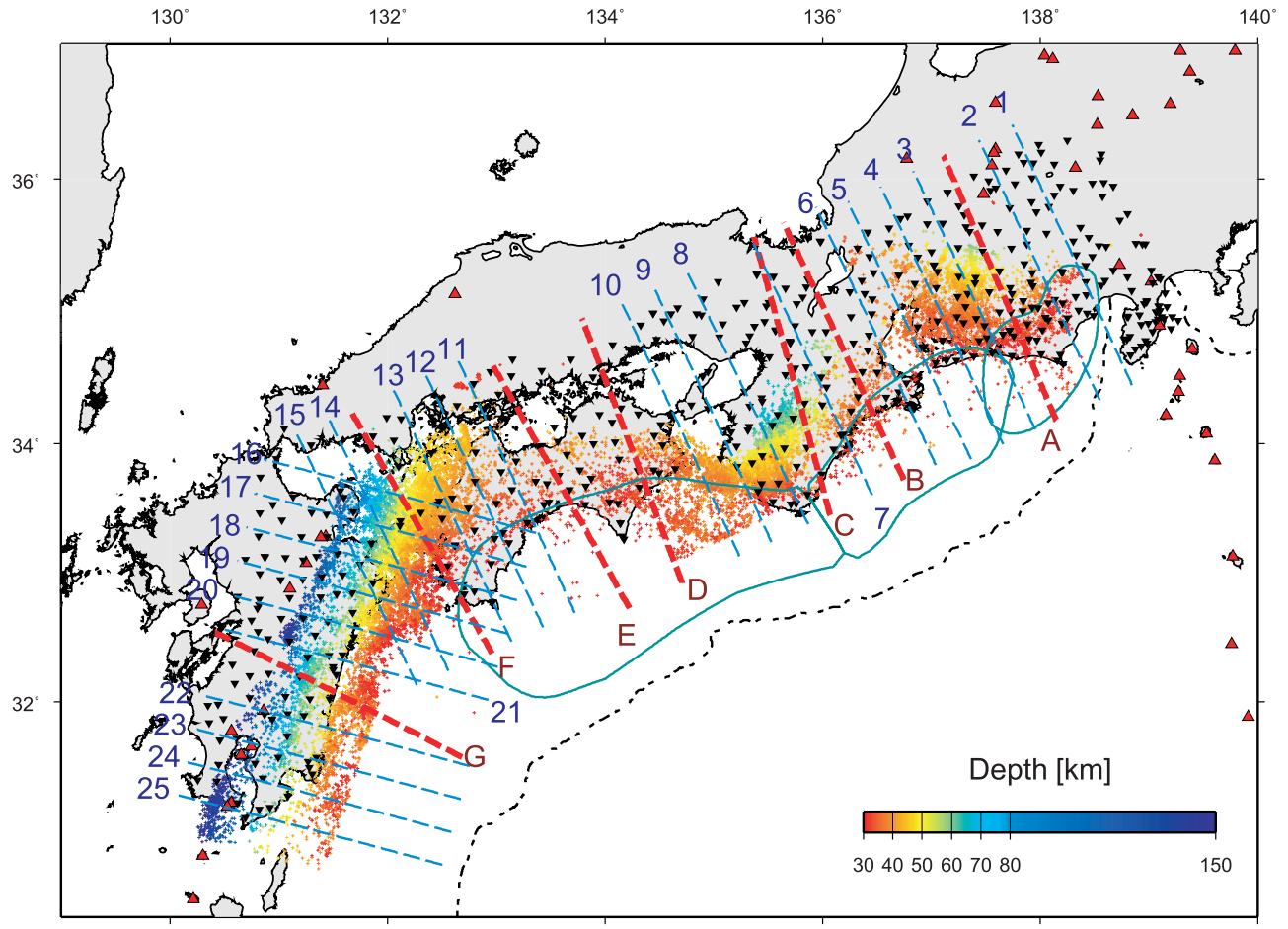

Figure 2. Epicenter distribution of earthquakes (crosses) at depths of 30–150 km and seismograph stations (solid reverse triangles) used in the double-difference tomography. Colors indicate the depth of hypocenters according to the color scale. Dashed blue lines show the locations of vertical cross sections 1 through 25 (see Figures 4–6). Dashed red lines denote the locations of vertical cross sections (A–G) for which the obtained velocity structures are compared with the results of seismic refraction surveys (Figures 7 and 9–14). Other symbols are the same as those in Figure 1.

probability that the upper envelope of intraslab earthquakes does not necessarily correspond to the plate boundary.

[4] In the present study, with the aim of deepening our understanding of the structure of the Philippine Sea plate, the double-difference (DD) tomography method [*Zhang and Thurber*, 2003] is employed to estimate the seismic velocity structure in a region from Tokai to southern Kyushu with precise hypocenter relocations. We then compare the 3-D velocity structure within the slab with the plate boundary of the Philippine Sea slab obtained from seismic reflection and refraction surveys [*Ichikawa et al.*, 1997; *Kodaira et al.*, 2000, 2002; *Nakanishi et al.*, 2002; *Takahashi et al.*, 2002; *Kodaira et al.*, 2004; *Ito et al.*, 2005] and the slab Moho obtained by receiver function analyses [*Yamauchi et al.*, 2003; *Shiomi et al.*, 2006], and also refer to focal mechanism solutions estimated by Japan Meteorological Agency (JMA) and this study, leading to a new model of plate boundary shape. Through these detailed investigations, the configuration and characteristics of the Philippine Sea plate are considered to be well resolved, providing very useful information on the seismotectonics of this region.

2. Data and Method

[5] In the DD tomography method [*Zhang and Thurber*, 2003], the difference of absolute traveltimes between pairs of earthquakes in close proximity are used in addition to the absolute traveltime data to constrain the velocity structure around hypocenteral regions. Rays from a pair of proximal earthquakes to a single seismograph station propagate on effectively identical propagation paths. By taking the difference of traveltimes between such a pair of earthquakes, the common error in the velocity structure along the two closely adjacent raypaths from the station could be removed. This permits the velocity structure in the vicinity of the hypocentral region to be estimated more accurately, yielding more accurate relative hypocenter positions. By performing this operation on all proximal pairs of earthquakes, it is possible to determine the relative hypocenters of many earthquakes over a wide area and to accurately

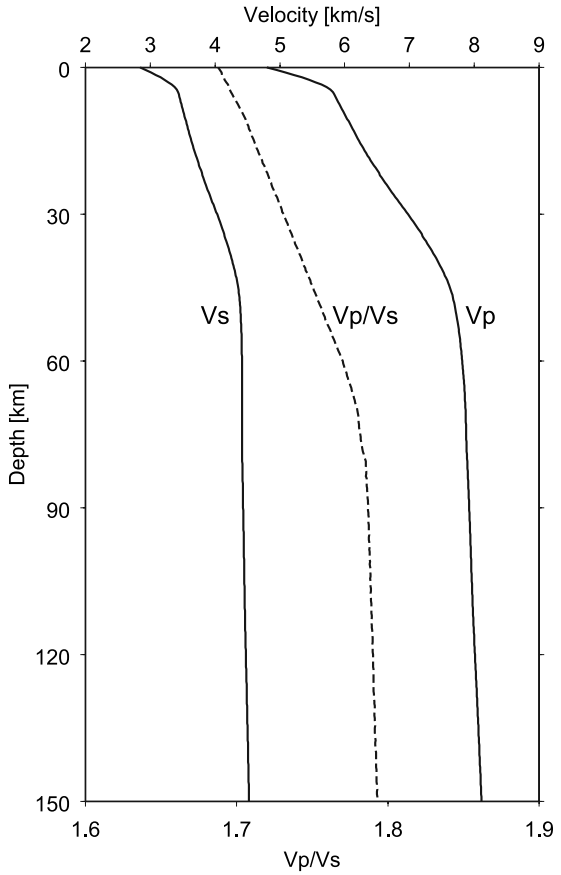

Figure 3. JMA2001 seismic velocity model [*Ueno et al.*, 2002] used in the initial velocity model in this study.

estimate the velocity structure in the hypocentral region. Note that the tomoFDD [*Zhang and Thurber*, 2006] is adopted in this study, which uses a finite difference traveltime algorithm taking the curvature of the Earth into consideration, because a lateral extent of the study area is at least 240 km × 240 km and hence the curvature of the Earth is not negligible.

[6] Arrival time data picked manually by the JMA, so-called a JMA-unified catalog, are used in this study. Approximately 8 years of data were analyzed, from 1 October 1997 to 31 December 2005, for the region from Tokai to southern Kyushu. Because of limitations on computational time and memory, the region was divided into five subregions, and the computations were performed separately for each region (regions a to e in Figure 1). Among the earthquakes recorded by 20 or more stations, all the earthquakes that occurred at depths of 20–150 km were included in the analysis (Figure 2, only at depths of 30–150 km), while earthquakes occurring at shallower depths that have a magnitude greater than M1.0 in regions a and d, and M1.5 in other regions were used. Earthquakes in oceanic regions, for which the accuracy of hypocenter determination is poor, and deep low-frequency earthquakes were not included in the analysis. The numbers of earthquakes, seismograph stations, differential traveltime data obtained from earthquake and station pairs, and absolute traveltime data used in the inversion in each region are given in Table 1. The distance between earthquake pairs was limited to 10 km in all regions. Grid intervals were set at 30–40 km along the direction of the Nankai Trough, 10–15 km in the direction perpendicular to it, and 5–10 km in the vertical direction (e.g., see Figure 7d). The initial velocity structure was given by the JMA2001 seismic velocity model [*Ueno et al.*, 2002] (Figure 3). Velocity discontinuities such as the continental Moho and plate boundary were not considered. Computations were continued for 8 iterations, yielding reduced root mean square (RMS) of traveltime residuals in each region, as shown in Table 1.

[7] The JMA determines focal mechanisms of earthquakes with magnitude of 3.2 or larger in land areas and 4.0 or above in oceanic regions from the polarity data of the first P wave arrival. As the earthquakes that occurred in the vicinity of the plate interface are generally small, the focal mechanism solutions for these earthquakes are not included in the JMA catalog. Therefore we collected waveforms of earthquakes occurring near the plate boundary and determined 581 focal mechanisms of small earthquakes with M $\geq$ 1.0 that are not included in the JMA catalog. The focal mechanisms determined in this study as well as those listed in the JMA catalog are taken into consideration to determine the upper plate interface of the Philippine Sea plate.

3. Results

3.1. Resolution Tests

[8] The reliability of the velocity images obtained by inversions can be checked by the checkerboard resolution tests (CRTs) [*Grand*, 1987; *Zhao et al.*, 1992]. Here, positive and negative velocity perturbations were assigned alternately to the grid points as an input model. Theoretical traveltimes between the hypocenters and stations were calculated for the same source-receiver geometry as the observations. Random noises corresponding to phase-picking errors were added to the theoretical traveltimes. Then, we inverted the synthetic traveltime data using an initial

Table 1. Data Sets Used in This Study and the Reduction of Root-Mean-Square Residuals of Traveltimes

		Area				
	Wave	a	b	c	d	e
Number of events		16,573	15,619	13,960	12,598	15,323
Number of stations		198	151	98	74	116
Number of absolute traveltimes	P	352,918	325,147	270,216	203,553	317,328
	S	344,848	327,204	262,814	210,394	308,111
Number of differential traveltimes	P	3,624,536	3,267,728	3,011,370	2,195,998	2,948,660
	S	3,580,950	3,229,343	2,836,181	2,329,858	2,996,051
RMS residuals of traveltimes (s)	P	0.12→0.09	0.10→0.07	0.10→0.06	0.12→0.10	0.14→0.11
	S	0.23→0.13	0.21→0.11	0.21→0.11	0.23→0.15	0.28→0.18

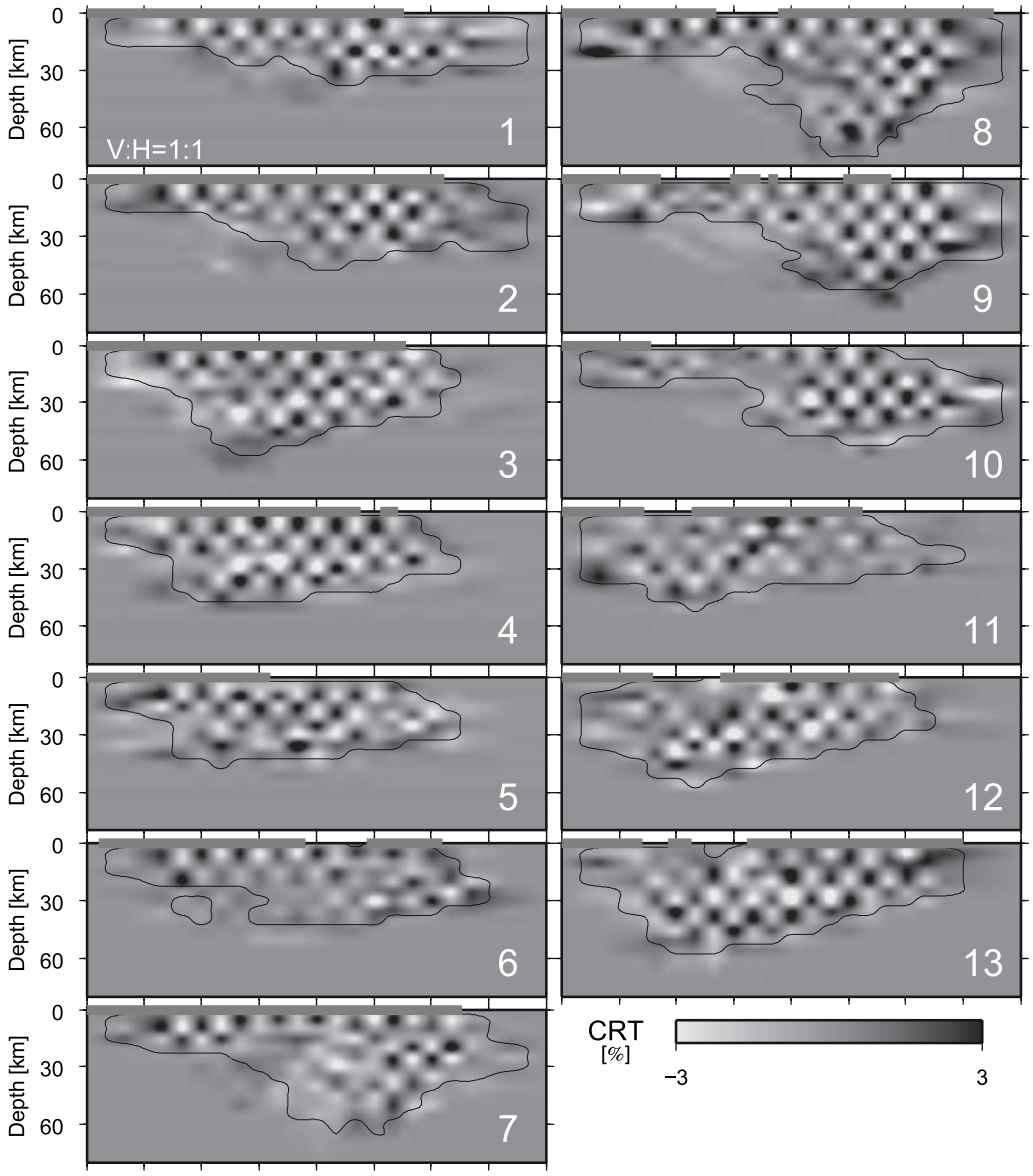

Figure 4. Vertical cross sections of CRTs for S wave velocity along lines 1–25 in Figure 2.

model without any velocity anomalies. If the pattern of velocity perturbations adopted in the input model is successfully reproduced, the solution is considered to be reliable.

[9] In the present research, ±3% disturbances were assigned to one grid point in horizontal and two adjacent grid points in vertical direction. Random errors with zero mean and standard deviation of 0.05 s for P wave, and zero mean and standard deviation of 0.1 s for S wave were added to the synthetic traveltime data. The CRT results of S wave are shown in Figure 4. It is apparent that the checkerboard patterns are generally recovered, and hence the solution is reliable. Narrow solid lines in Figure 4 denote the derivative-weighted summations [*Thurber and Eberhart-Phillips*, 1999], which is an indicator for the ray density distribution (3000 contours are shown). Within these solid lines, the results of CRTs show good recovery, and the reliability of the solutions is considered to be relatively high. Although the western part of the cross sections 18 to 25 shows discrepancy between the high-recovery area of CRTs and the area of dense raypath coverage, the results of CRTs show good resolution around source regions of intraslab seismicity, which confirms the validity of estimation of the plate boundary from the obtained seismic velocity structure.

3.2. Seismic Wave Velocity Structure in and Around the Philippine Sea Slab

[10] Vertical cross sections of S wave velocity (Vs) perturbations (in %) relative to the JMA2001 [*Ueno et al.*, 2002] are shown in Figure 5 for observation lines 1 to 25 in Figure 2. In all of the cross sections, it is clear from the distribution of hypocenters that the Philippine Sea slab is subducting beneath the land area. Most of the intraslab earthquakes are distributed below a low-velocity layer of up to several kilometers in thickness. Furthermore, along

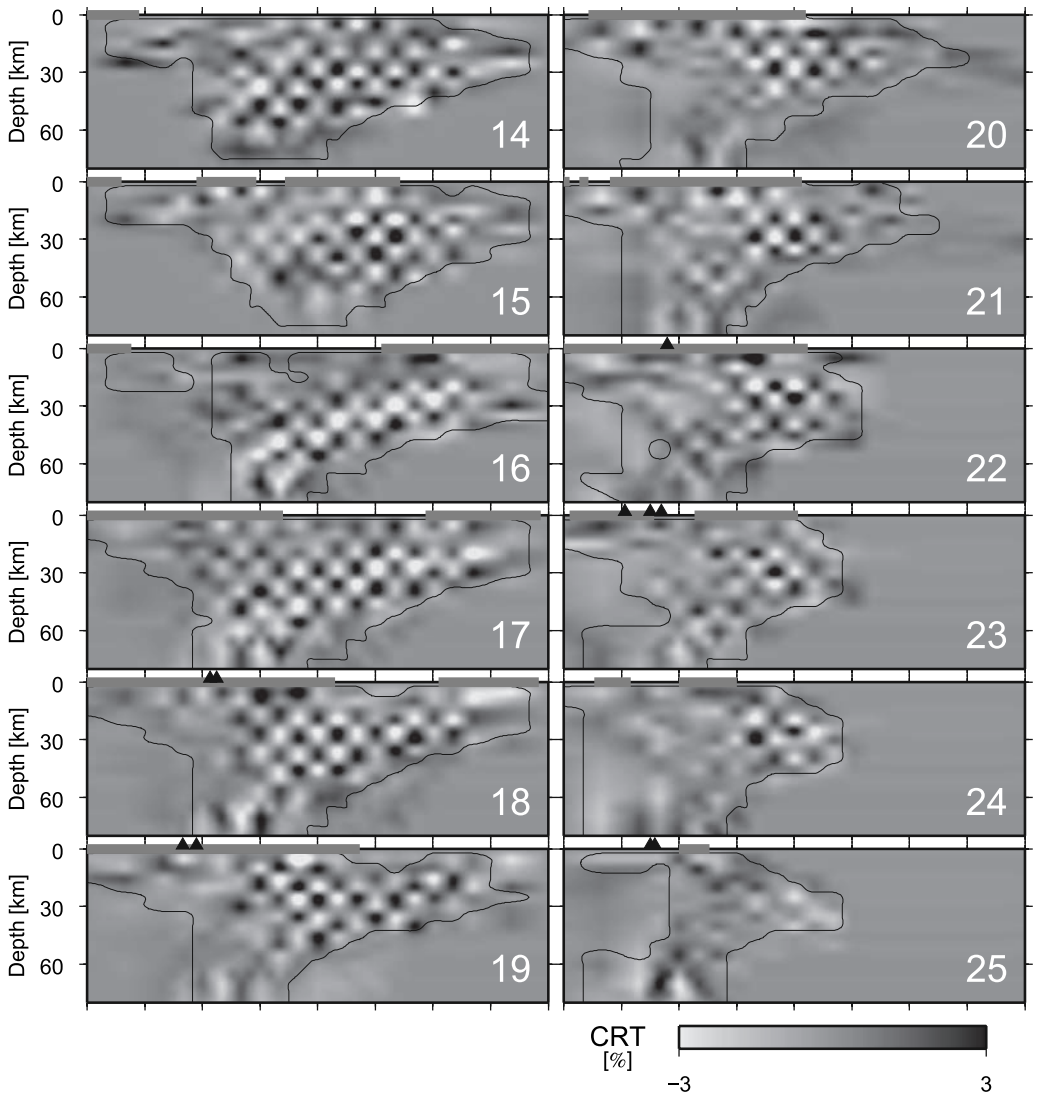

Figure 4. (continued)

observation line 15 and subsequent lines, low-Vs anomalies are distributed in the mantle wedge. Solid red lines in Figure 5 represent the plate boundaries, which will be estimated in section 4. The area enclosed by a rectangle in observation lines 16 to 22 in the Kyushu region is shown enlarged in Figure 17, which will be discussed in section 4. Earthquakes between purple arrows denote the lower plane of the double seismic zone on panels 4–10, 12–15, 17–18, and 21–24. Note that the velocity structure of P wave is generally similar to that of S wave and hence only S wave velocity structures are shown in Figure 5. However, the P wave velocity structure along major seven lines is shown in Figures 7 and 9–14.

[11] The perturbations of ratios of P wave to S wave velocity (Vp/Vs) in vertical cross sections along observation lines 1 to 25 are shown in Figure 6. A zone of high-Vp/Vs ratios in thickness of several kilometers is distributed immediately above intraslab earthquakes (see lines 3–5, 7–14, 16, 18, 19, and 25). High-Vp/Vs anomalies imaged in the mantle wedge of observation lines 15–25 are characteristic features in Kyushu as described later.

3.3. Comparison of 3-D Velocity Structures With Results of Reflection and Refraction Seismic Surveys and Receiver Function Analyses

[12] The results of DD tomography along observation line A in Figure 2 are shown in Figure 7. The trends of distributions of P wave (Figure 7a) and S wave velocity perturbations (Figure 7b) are similar to each other. A low-Vs and high-Vp/Vs layer of several kilometers in thickness exists immediately above the region of high seismic activity (Figure 7c). Superimposing the plate boundary (black solid line) obtained from a seismic reflection and refraction survey performed along this line [*Kodaira et al.*, 2004], nearly exact agreement can be seen with the upper limit of the above mentioned low-Vs and high-Vp/Vs layer. In addition, the slab Moho estimated by receiver function analysis [*Shiomi et al.*, 2006] is located below this low-Vs and high-Vp/Vs layer. It is thus inferred that the low-Vs and

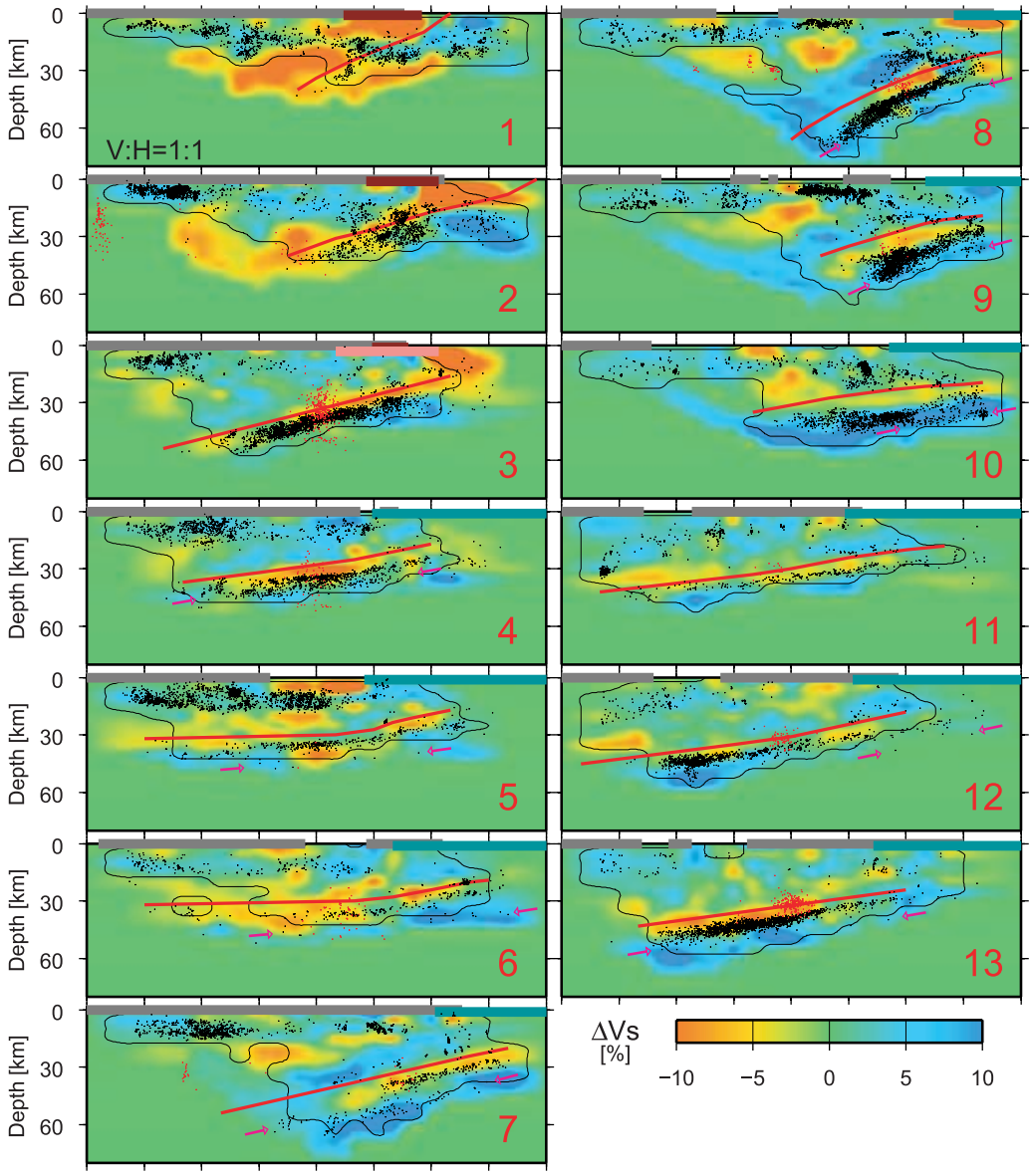

Figure 5. Vertical cross sections of S wave velocity perturbations (in %) relative to the JMA2001 [*Ueno et al.*, 2002] along lines 1–25 in Figure 2. Red lines denote the location of plate boundary estimated in this study. Black and red crosses denote earthquakes relocated by double-difference tomography and deep low-frequency earthquakes, respectively, within a 3 km wide zone for lines 13 and 14 and a 15 km wide zone for other lines. Thick gray line at the top of panels denotes the land area, brown lines denote surface locations of estimated locked zone or asperities [*Matsumura*, 1997; *Yagi et al.*, 1998], pink lines denote surface locations of long-term slow slip events [*Hirose et al.*, 1999; *Ozawa et al.*, 2001, 2002; *Miyazaki et al.*, 2006], and blue lines denote expected source region of Tonankai earthquake and Nankai earthquake (Earthquake Research Committee, Long-term evaluation of earthquakes in the Nankai trough, 2001, available at http://www.jishin.go.jp/main/chousa/01jun_kitakami/index.htm). Red triangles represent active volcanoes, and thin black lines represent a DWS (derivative-weighted summations) of 3000 [*Thurber and Eberhart-Phillips*, 1999]. Rectangles on plots of lines 16–22 show the area magnified in Figure 17. Purple arrows on plots of lines 4–10, 12–15, 17–18, and 21–24 indicate the lower plane seismicity of the double seismic zone.

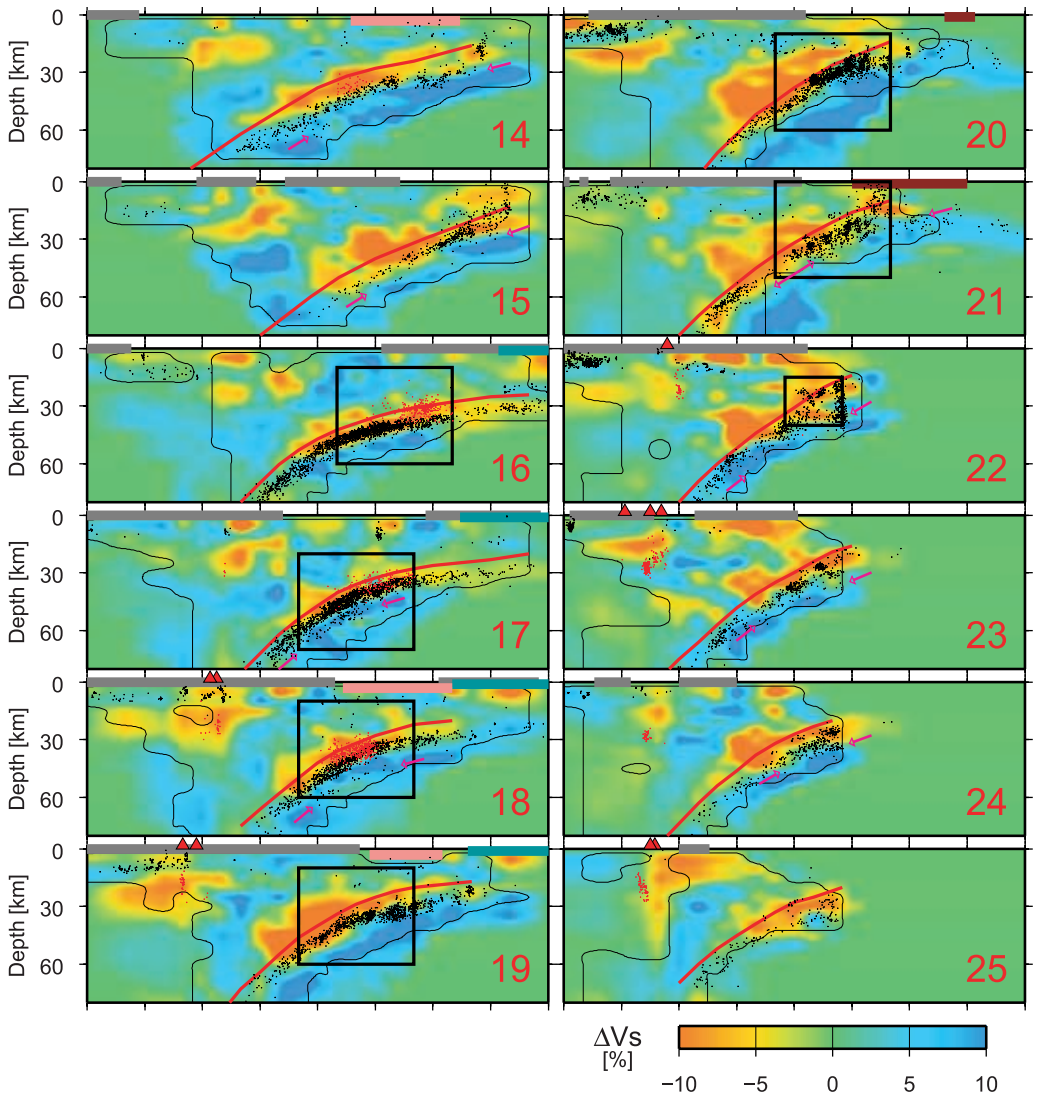

Figure 5. (continued)

high-Vp/Vs layer corresponds to the oceanic crust and the upper interface of the Philippine Sea slab is delineated as a red curve in Figure 7c. The black dashed line denotes the continental Moho [*Kodaira et al.*, 2004], which corresponds to the contour of Vp = 7.0 km/s. The contour of Vp of 7.0 km/s obtained in the present analysis, shown as a red dashed line in Figure 7a, is consistent with the velocity structure of *Kodaira et al.* [2004].

[13] Difference in the assumed velocity model should be taken into consideration when comparing the plate boundary positions estimated from seismic reflection and refraction surveys with the hypocenters of natural earthquakes, since the hypocenter locations vary depending on the assumed seismic velocity structure. For intercomparison, a horizontally stratified structure is constructed from the P wave velocity structure obtained by *Kodaira et al.* [2004], and hypocenters are relocated for that model only using P wave absolute traveltimes. The hypocenters of earthquakes thus relocated along line A are shown in Figure 8. Although hypocenters of intraslab earthquakes became somewhat shallower after the relocation, there exists a several kilometer gap between the plate boundary surface estimated by *Kodaira et al.* [2004] and the upper limit of intraslab earthquakes. These results suggest the validity of a direct comparison of the plate boundary surface estimated by reflection and refraction surveys with the distribution of intraslab earthquakes.

[14] Vertical cross sections of perturbations of Vp, Vs, and Vp/Vs along survey line B in Figure 2 are shown in Figure 9. Here, as in the vertical cross section along survey line A (Figure 7), a low-Vs and high-Vp/Vs layer of several kilometers in thickness can be seen immediately above the seismically active region in the slab. The slab Moho surface obtained by receiver function analyses (green solid line, *Yamauchi et al.* [2003], and purple solid line, *Shiomi et al.* [2006]) are superimposed in Figure 9. As these surfaces closely follow the lower limit of the low-Vs and high-Vp/Vs layer with a several kilometer thickness, this layer is inferred to correspond to the oceanic crust, with the plate boundary drawn through its

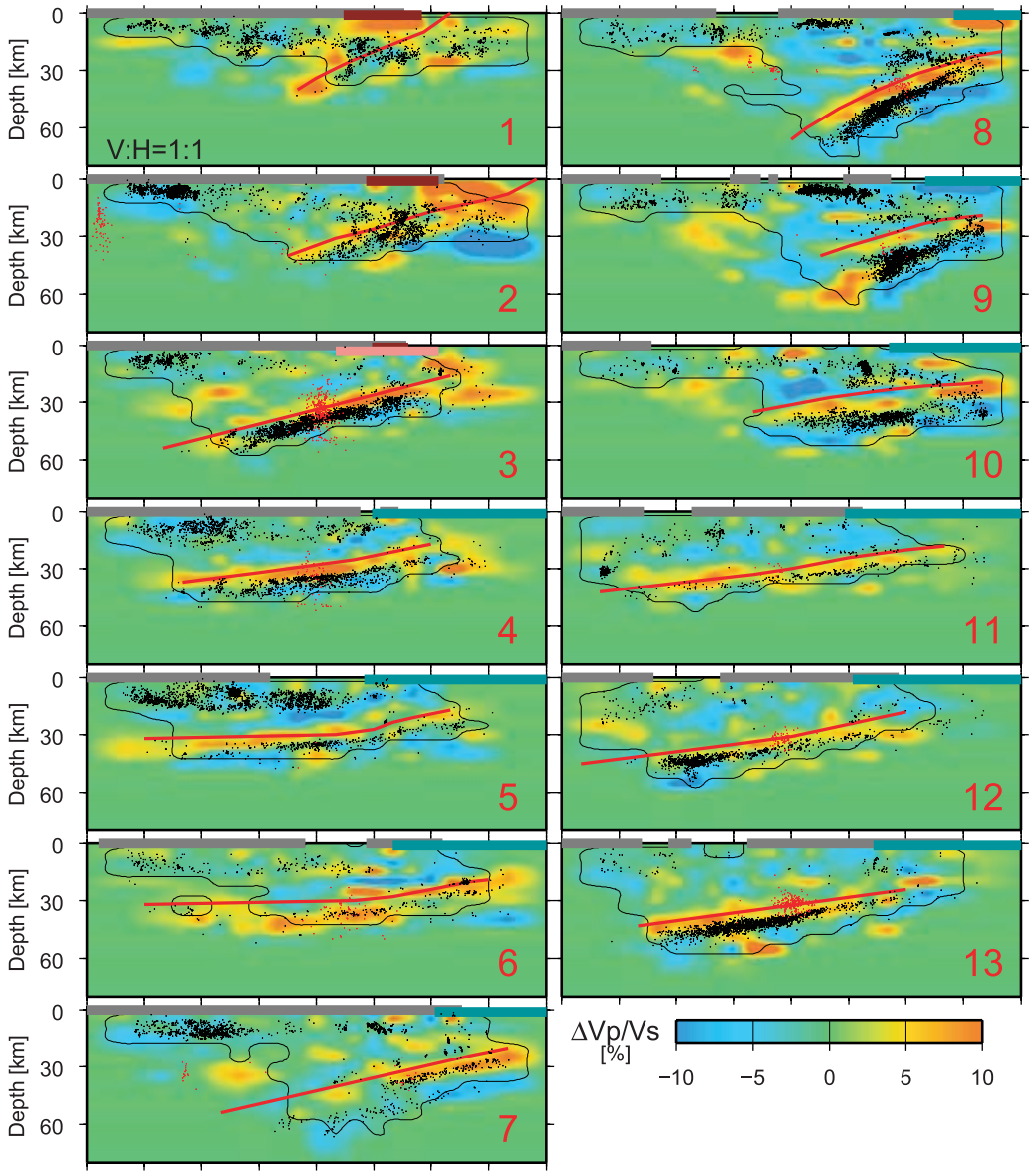

Figure 6. Vertical cross sections of Vp/Vs ratio perturbations along lines 1–25 in Figure 2. Symbols are the same as those in Figure 5.

upper limit (red solid line in Figure 9c). A seismic reflection and refraction survey conducted along the seaward extension of this line [*Nakanishi et al.*, 2002] determined the plate boundary at depths shallower than 20 km as shown by a black line. The shallower extension of the plate boundary estimated in this study is consistent with that estimated by *Nakanishi et al.* [2002].

[15] Figure 10 shows vertical cross sections of perturbations of Vp, Vs, and Vp/Vs along observation line C in Figure 2. A low-Vs layer of several kilometers in thickness is again seen directly above the seismically active region in the slab. Although a distinct low-Vs and high-Vp/Vs layer is imaged immediately above it along lines 7 and 8, which are located in both sides of line C, a high-Vp/Vs layer is not apparent in line C. We have no idea why the high-Vp/Vs layer is not clear in line C, but it might be related to an abrupt change in the slab shape in this region. Small-scale variation in heterogeneous structure beneath the Kii peninsula needs to be investigated in future studies. The plate boundary obtained from reflection and refraction seismic survey carried out along this observation line ([black solid line, *Ito et al.* [2005]) and the slab Moho obtained from receiver function analyses (green solid line, *Yamauchi et al.* [2003], and purple solid line, *Shiomi et al.* [2006]) are superimposed in Figure 10. The low-Vs and high-Vp/Vs layer, inferred to correspond to oceanic crust, is distributed at depths of 30–40 km, sandwiched between the plate boundary and slab Moho. Deeper than 45 km, the plate boundary estimated from seismic reflection and refraction surveys and the slab Moho surface estimated from the receiver function intersect in some places and become superimposed in others, which might be due to an abrupt

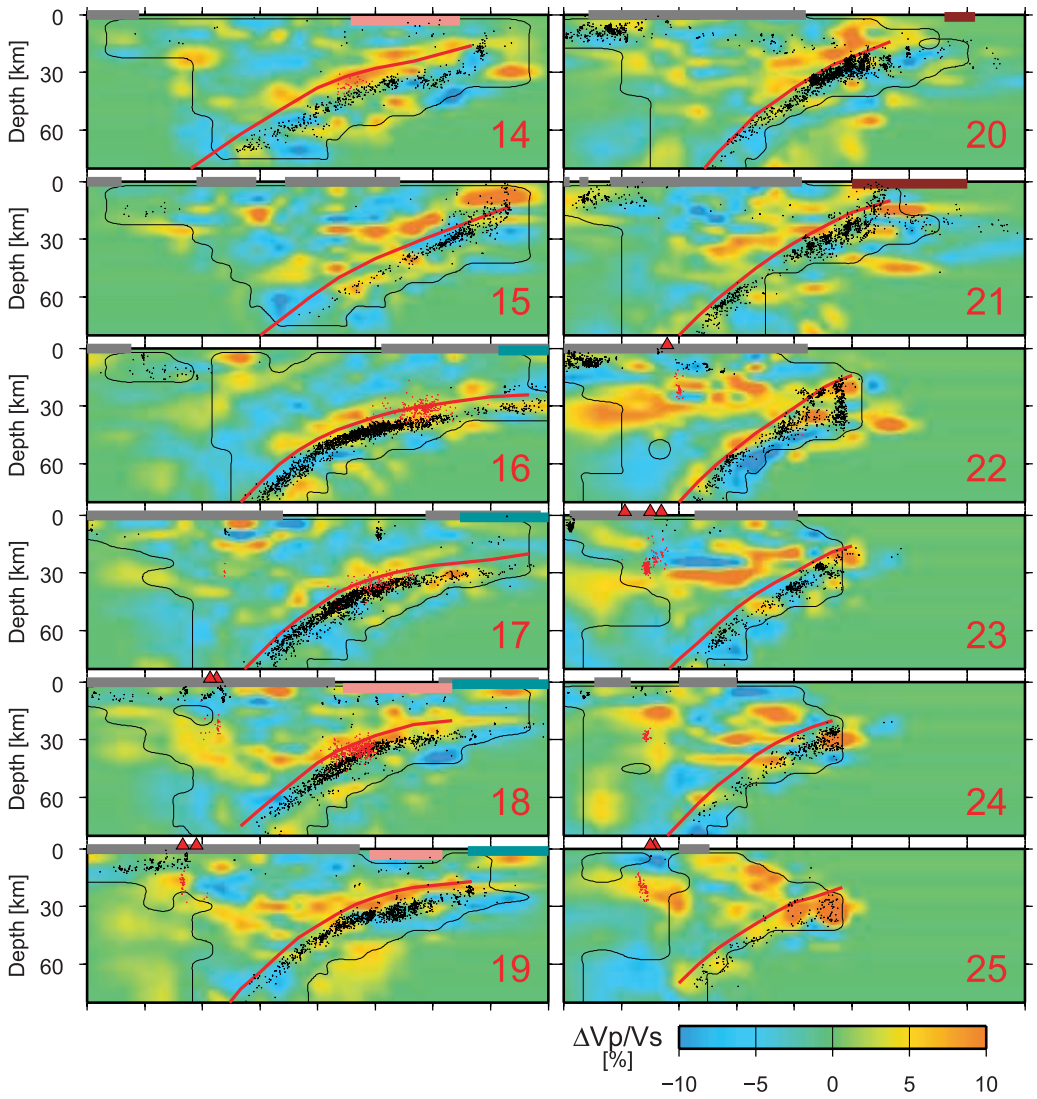

Figure 6. (continued)

change in the dip of the Philippine Sea slab beneath the Kii Peninsula (see lines 7 to 9 in Figures 5 and 6).

[16] Likewise in the other cross sections, a low-Vs and high-Vp/Vs layer of several kilometers in thickness is distributed above the seismically active region within the slab in eastern Shikoku (Figures 11 and 12), although slab earthquakes tend to occur at a constant depth of ~30 km in Figure 11 in contrast to the inclined plate boundary and slab Moho. We consider that the hypocenters of slab earthquakes tend to concentrate around a constant depth of ~30 km. One is the uncertainty in relocation of offshore earthquakes. The other is that offshore earthquakes may consist of the lower plane seismicity of the double seismic zone, as shown by purple arrows in Figure 11a. That is why the low-Vs and high-Vp/Vs layer is not distributed directly above the offshore seismically active region in Figure 11. A low-Vs and high-Vp/Vs layer is again sandwiched between the plate boundary [*Kodaira et al.*, 2000, 2002] and slab Moho surfaces (green solid line, *Yamauchi et al.* [2003], and purple solid line, *Shiomi et al.* [2006]). *Shelly et al.* [2006] investigated the detailed seismic velocity structures using waveforms of low-frequency earthquakes in western Shikoku by DD tomography and revealed the existence of a low-Vs and high-Vp/Vs layer of several kilometers in thickness, indicative of high pore water pressure. Their precise relocation of hypocenters suggests that low-frequency earthquakes occur immediately above the layer on a surface inclined to the north while intraslab earthquakes are distributed below it. They interpreted the interface on which low-frequency earthquakes are distributed to be the plate boundary, consistent with the results of this study.

[17] Figure 13 shows that a low-Vs layer with a several kilometer thickness exists in and above the intraslab earthquakes in the Bungo Channel, but a zone of high-Vp/Vs ratio with a several kilometer thickness lies immediately above the low-Vs layer, in contrast with the results for the other lines described above. It appears that the plate boundary obtained by seismic reflection and refraction survey conducted along this line (black solid line, *Takahashi et al.*

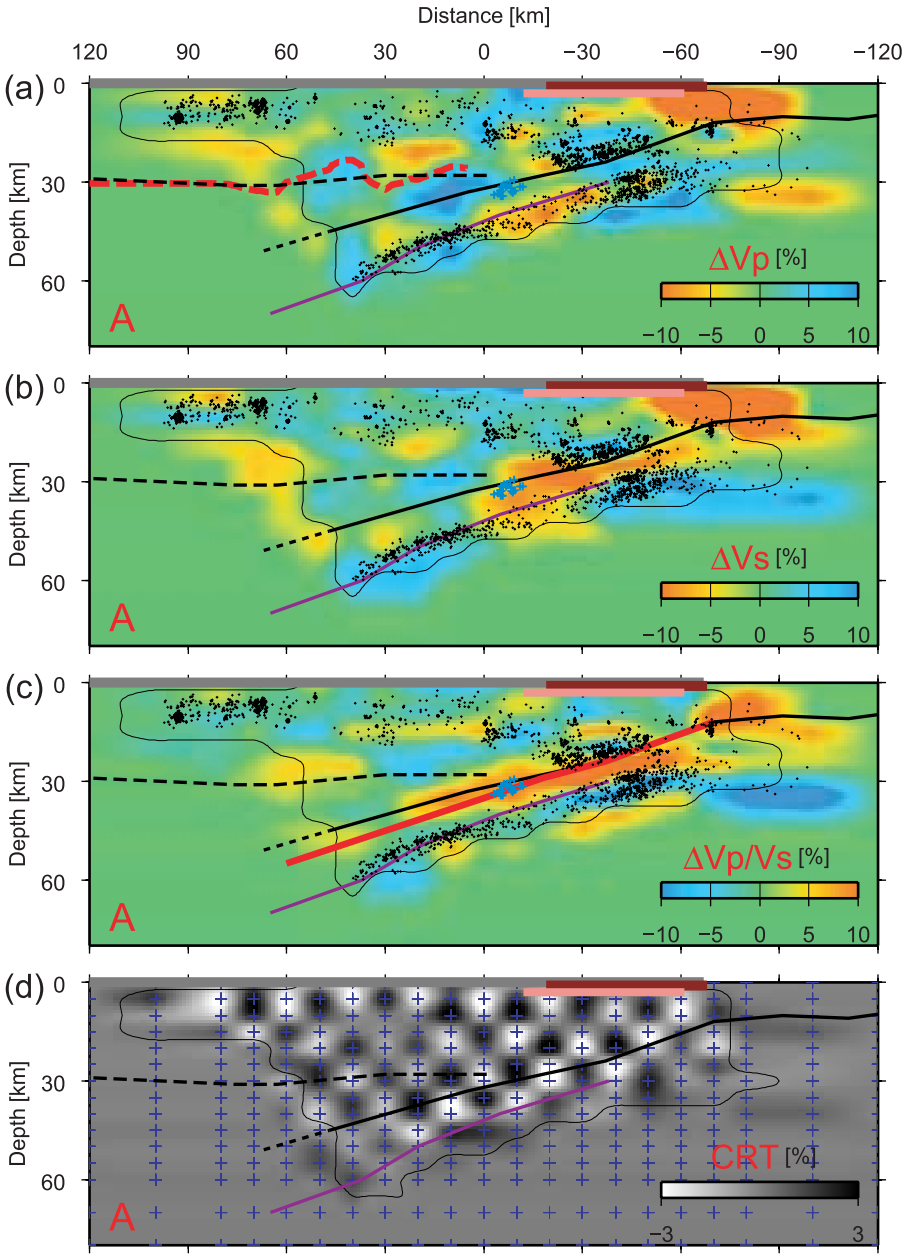

Figure 7. Vertical cross sections of (a) P wave and (b) S wave velocity perturbations, (c) Vp/Vs ratio perturbations, and (d) CRTs for S wave velocity along line A in Figure 2. Red line in Figure 7c shows the estimated location of the plate boundary. Solid black lines denote the plate boundary estimated by seismic reflection and refraction survey [*Kodaira et al.*, 2004], purple lines denote the slab Moho imaged by receiver function analysis [*Shiomi et al.*, 2006], and dashed lines denote the island arc Moho [*Kodaira et al.*, 2004]. Dashed red line in Figure 7a represents a velocity contour of 7.0 km/s estimated in this study. Light blue crosses in Figures 7a–7c denote relocated nonvolcanic deep low-frequency earthquakes (see section 5.3 for details). Blue crosses in Figure 7d denote grid points adopted in inversion. Other symbols are the same as those in Figure 5.

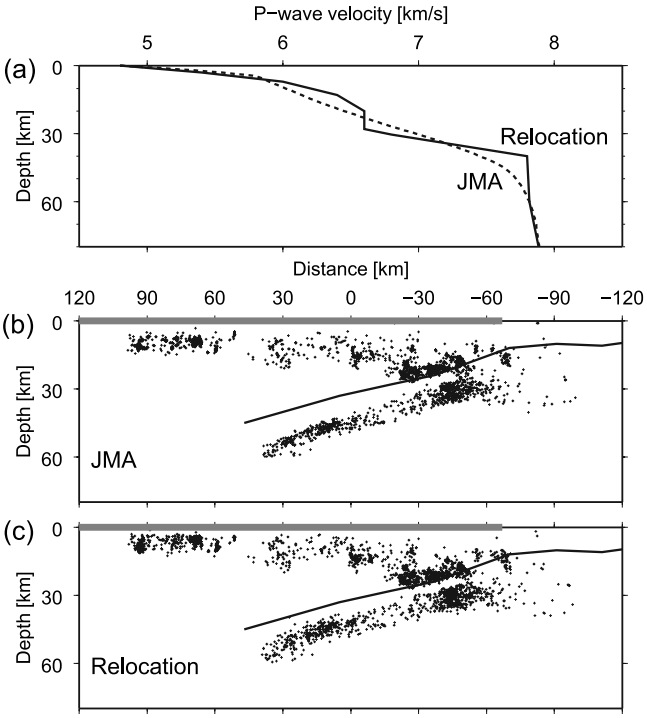

Figure 8. (a) P wave velocity structure used in hypocenter relocation (solid line) and that used by the JMA (dashed line). A simplified model based on P wave velocity structure by *Kodaira et al.* [2004], at a horizontal distance of −30 km in Figure 8b, is used for relocation. Vertical cross sections of hypocenter locations determined by (b) the JMA and (c) the present study along line A in Figure 2. Note that only absolute traveltimes of P wave are used in the relocation.

[2002]) corresponds to the shallower extension of the low-Vs layer. The slab Moho estimated by receiver function analysis [*Shiomi et al.*, 2006] is located subparallel to the plate boundary determined by *Takahashi et al.* [2002] at a depth around 30 km with an offset of 7–10 km from the plate boundary. Assuming that the low-Vs layer sandwiched between the plate boundary and the slab Moho is an oceanic crust, we delineate the plate boundary in this region (red line in Figure 13c) so as to connect to the plate boundary determined by refraction survey (black line) at shallower depths.

[18] A low-Vs and high-Vp/Vs layer of several kilometers in thickness exists above the intraslab earthquakes in Kyushu (Figure 14). The high-Vp/Vs anomaly in the mantle wedge have been revealed by previous studies and interpreted to be caused by serpentinization of mantle peridotite [*Honda and Nakanishi*, 2003; *Wang and Zhao*, 2006]. The plate boundary obtained by seismic reflection and refraction survey along this observation line [*Ichikawa et al.*, 1997] is limited below the Pacific Ocean and it is difficult to refer to it to delineate the plate boundary beneath the land area.

[19] A prominent low-Vs region exists in the mantle wedge along observation lines 15 to 24 in the region from the Bungo Channel to southern Kyushu (Figure 5), where Vp/Vs values are partly high (Figure 6). This feature makes it difficult to discern the low-Vs and high-Vp/Vs signature of oceanic crust. Therefore, focal mechanism solutions of intraslab earthquakes are additionally referred to estimate the location of the plate boundary, as described in the next chapter.

4. Configuration of the Upper Plate Interface of the Philippine Sea Slab

[20] As discussed in details in section 3, comparison of the velocity structures obtained by DD tomography, the plate boundary surface obtained by seismic refraction surveys, and the slab Moho surfaces obtained by receiver function analyses indicates that the low-Vs and high-Vp/Vs layer corresponds to the oceanic crust of the subducted Philippine Sea slab. Figures 5 and 6 show that this several kilometer thick layer of low-Vs and high-Vp/Vs is distributed throughout most of the region and intraslab earthquakes mainly occur below or the lower part of the layer. This is a characteristic feature seen in SW Japan, except for Kyushu, associated with the subduction of the Philippine Sea slab.

[21] In the previous section, we interpret the low-Vs and high-Vp/Vs layer above intraslab earthquakes to be the subducting oceanic crust and delineate the upper plate interface of the subducting Philippine Sea slab along the upper limit of the layer. According to the phase diagram and the thermal model for Nankai, SW Japan, estimated by *Hacker et al.* [2003], P and S wave velocities of the oceanic crust are 7.1–7.3 km/s and 3.9–4.1 km/s, respectively, for hydrous minerals at depths of 20–40 km under the assumption that the entire crust is composed of fully hydrated MORB. The absolute velocities of the oceanic crust observed in this study range 6.9 ± 0.4 km/s in P waves and 3.9 ± 0.2 km/s in S waves at depths of 20–40 km. Although P wave velocities observed in this study are consistent with those obtained by the seismic reflection and refraction surveys [*Kodaira et al.*, 2000, 2002; *Nakanishi et al.*, 2002; *Takahashi et al.*, 2002; *Kodaira et al.*, 2004] (Figure 15a), P and S wave velocities are slightly lower than those estimated by *Hacker et al.* [2003]. Figure 15 shows that the observed Vp/Vs values in the oceanic crust are scattered in a range of 1.79 ± 0.09 but are comparable to those listed in *Hacker et al.* [2003], in which the Vp/Vs values in the oceanic crust are considered to be ∼1.79 at depths of 20–40 km for the P-T path of Nankai. The differences between the P and S wave velocities observed in this study and those expected from *Hacker et al.* [2003] can be qualitatively explained if thermal structure in the Philippine Sea slab would be higher than the model by *Hacker et al.* [2003], even though the possible ambiguity of thermal structure and phase diagram as well as the uncertainty in the observed velocity values should be considered for quantitative comparison.

[22] For Tokai and Kyushu, we referred to the distribution of low-angle thrust-type earthquakes in addition to that of a low-Vs and high-Vp/Vs layer to delineate the upper interface of the Philippine Sea slab. *Matsumura* [1997] estimated the position of the asperity region (locked region) for the Tokai earthquake based on microearthquake activity within the slab and the distribution of P axis of focal mechanisms. An aseismic region with a thickness of 5–10 km is observed between seismicity in the continental plate and

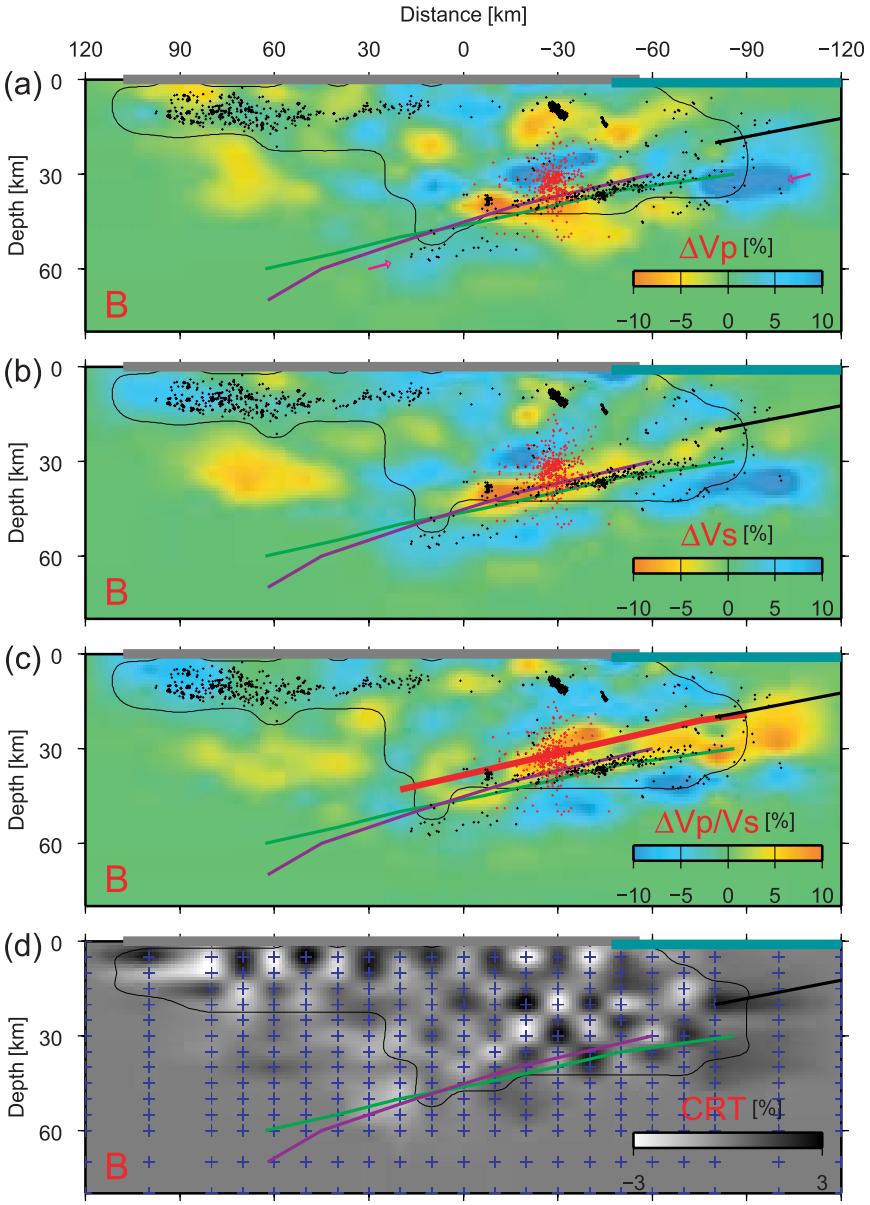

Figure 9. Vertical cross sections of (a) P wave and (b) S wave velocity perturbations, (c) Vp/Vs ratio perturbations, and (d) CRTs for S wave velocity along line B in Figure 2. Solid black lines denote the plate boundary estimated by seismic reflection and refraction survey [*Nakanishi et al.*, 2002], and green and purples lines denote slab Moho imaged by receiver function analyses by *Yamauchi et al.* [2003] and *Shiomi et al.* [2006], respectively. Purple arrows in Figure 9a indicate the seismicity of the lower seismic plane. Other symbols are the same as those in Figure 5.

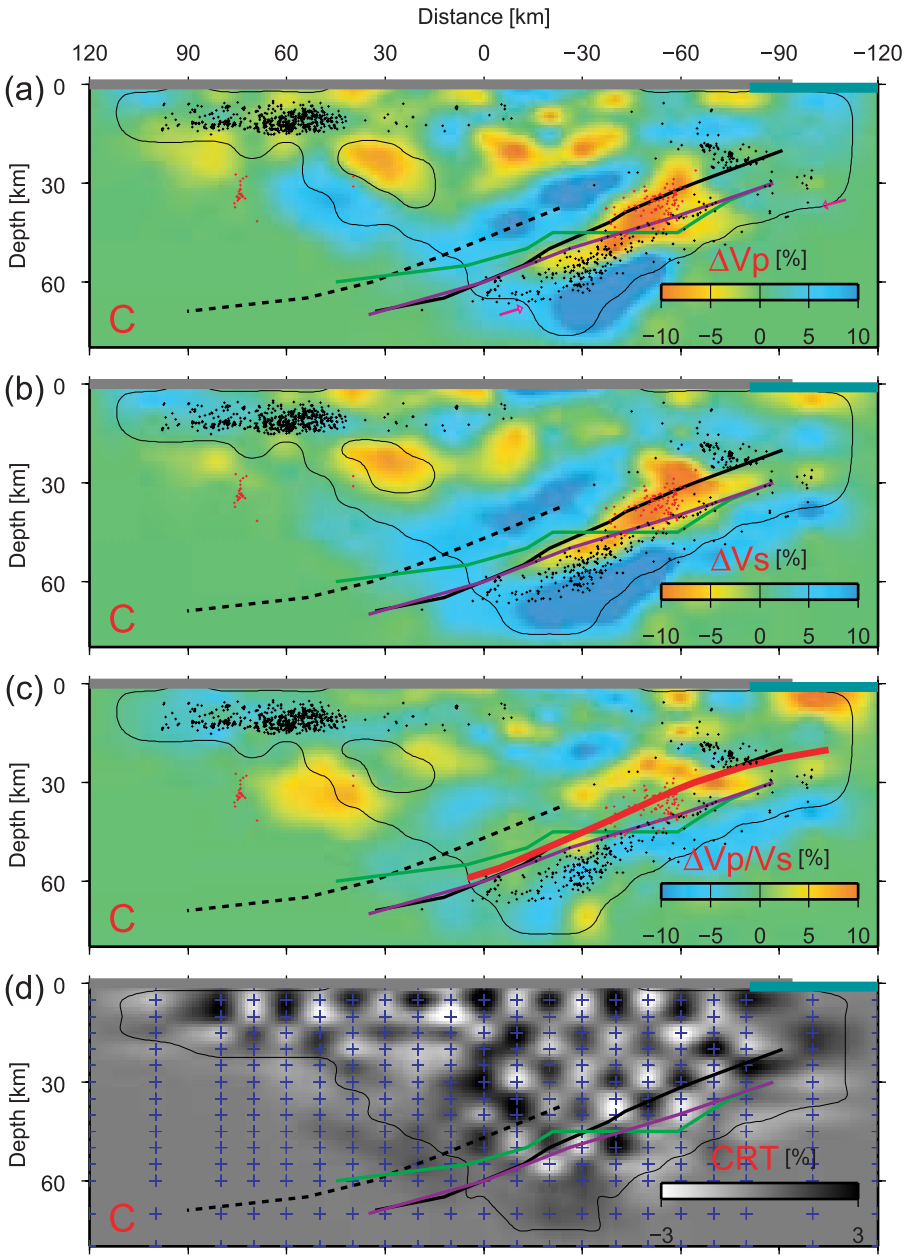

Figure 10. Vertical cross sections of (a) P wave and (b) S wave velocity perturbations, (c) Vp/Vs ratio perturbations, and (d) CRTs for S wave velocity along line C in Figure 2. Solid and dashed black lines denote the plate boundary and another reflection plane estimated by seismic reflection and refraction survey [*Ito et al.*, 2005], respectively. Other symbols are the same as those in Figures 5 and 9.

subducted Philippine Sea plate. This aseismic region is thus considered to correspond to locked portion of both plates. Figure 16 shows five vertical cross sections of perturbations of Vs, Vp/Vs, and P and T axes of the focal mechanism across the locked portion proposed by *Matsumura* [1997]. A prominent low-Vs and high-Vp/Vs layer is seen in lines c to e, and thus it is possible that the upper plate interface is delineated above the layer in the same manner as in Figure 7. Moreover, the precise relocation of hypocenters by DD algorithm reveals an isolated and rather clustered seismicity within the seismic gap, and some events in the isolated clusters have low-angle thrust-type focal mechanism solutions. We delineate the plate boundary in Tokai by taking into account these low-angle thrust-type earthquakes as well as the distribution of the low-Vs and high-Vp/Vs layer as shown in Figure 16.

[23] The focal mechanism solutions of earthquakes that occurred beneath Kyushu are plotted in Figure 17. It is apparent that focal mechanisms of intraslab earthquakes beneath Kyushu exhibit mostly downdip extensional type with a principal tension axis in the direction of subduction [e.g., *Wang et al.*, 2004]. However, low-angle thrust-type earthquakes are also observed along observation lines 20, 21, and G. These events are important indicators to deduce the plate boundary and used as references to estimate the location of the plate boundary. Along line 22, there exists an

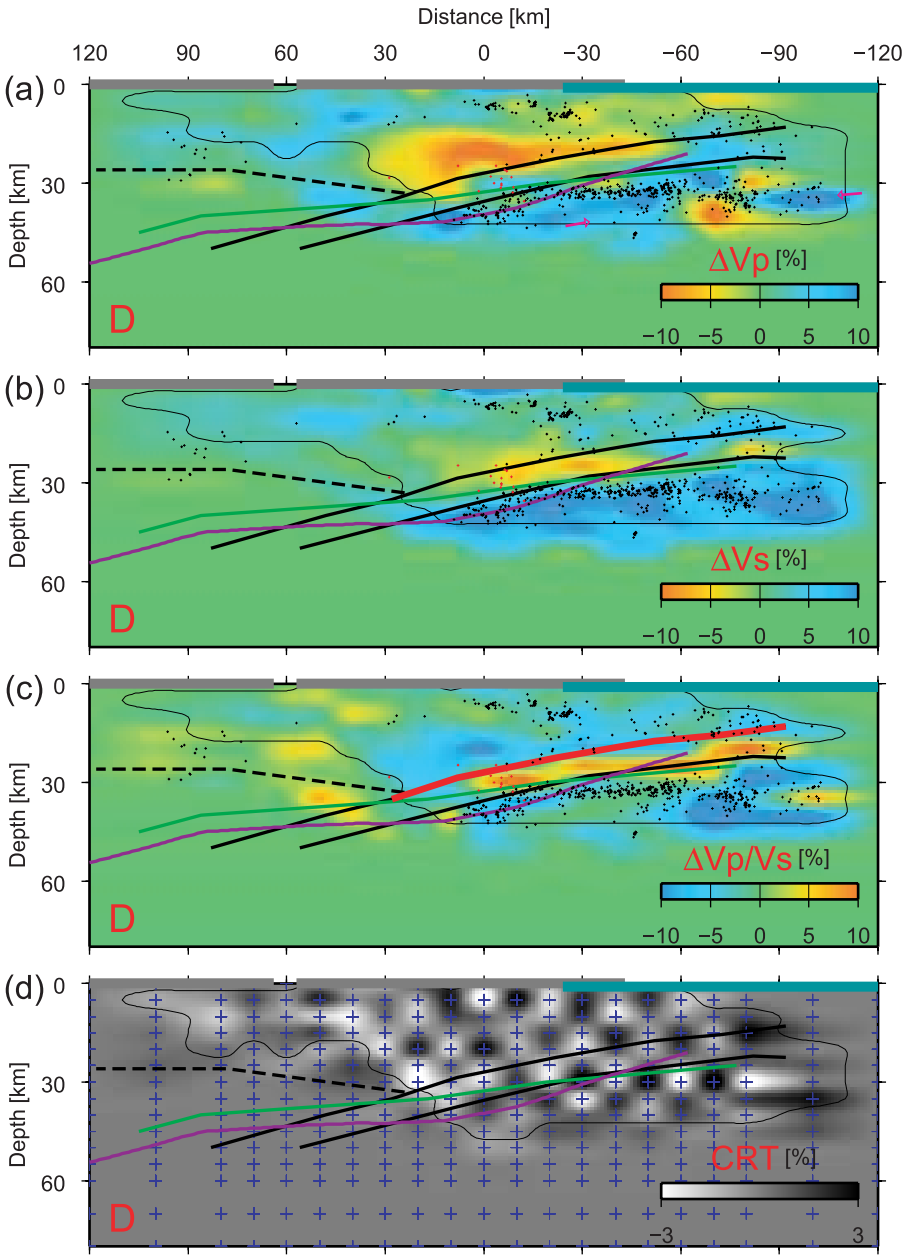

Figure 11. Vertical cross sections of (a) P wave and (b) S wave velocity perturbations, (c) Vp/Vs ratio perturbations, and (d) CRTs for S wave velocity along line D in Figure 2. Solid black lines denote the plate boundary and the slab Moho estimated by seismic reflection and refraction survey [*Kodaira et al.*, 2002], and dashed lines denote the island arc Moho [*Kodaira et al.*, 2002]. Other symbols are the same as those in Figures 5 and 9.

earthquake cluster sloping downward toward the east (Figure 17, right) at depths of 25–30 km. As the focal mechanism solutions of these earthquakes are quite different from those of earthquakes occurring immediately below the cluster, we infer that the plate boundary is placed between the two locations. Along the remaining observation lines, the plate boundary is estimated to be located above the region of low Vs (with high-Vp/Vs as a supplementary indicator) around a depth of 30 km, and we extend the plate boundary smoothly to the deeper depths with taking also into account intraslab seismic distribution.

[24] The plate boundary estimated in this study is shown by the contours in Figure 18. It is noted that considering the distributions of hypocenters and seismograph stations used in this study, the estimated location of the plate boundary is limited to a depth range of 20–50 km. For the region shallower than 20 km, the compiled results of *Baba et al.* [2002] based on oceanic air gun surveys are referred to the position of the plate boundary. At depths greater than 50 km, the plate boundary estimated by *Nakajima and Hasegawa* [2007] is used. Isodepth contours of the plate boundary are drawn at 10 km

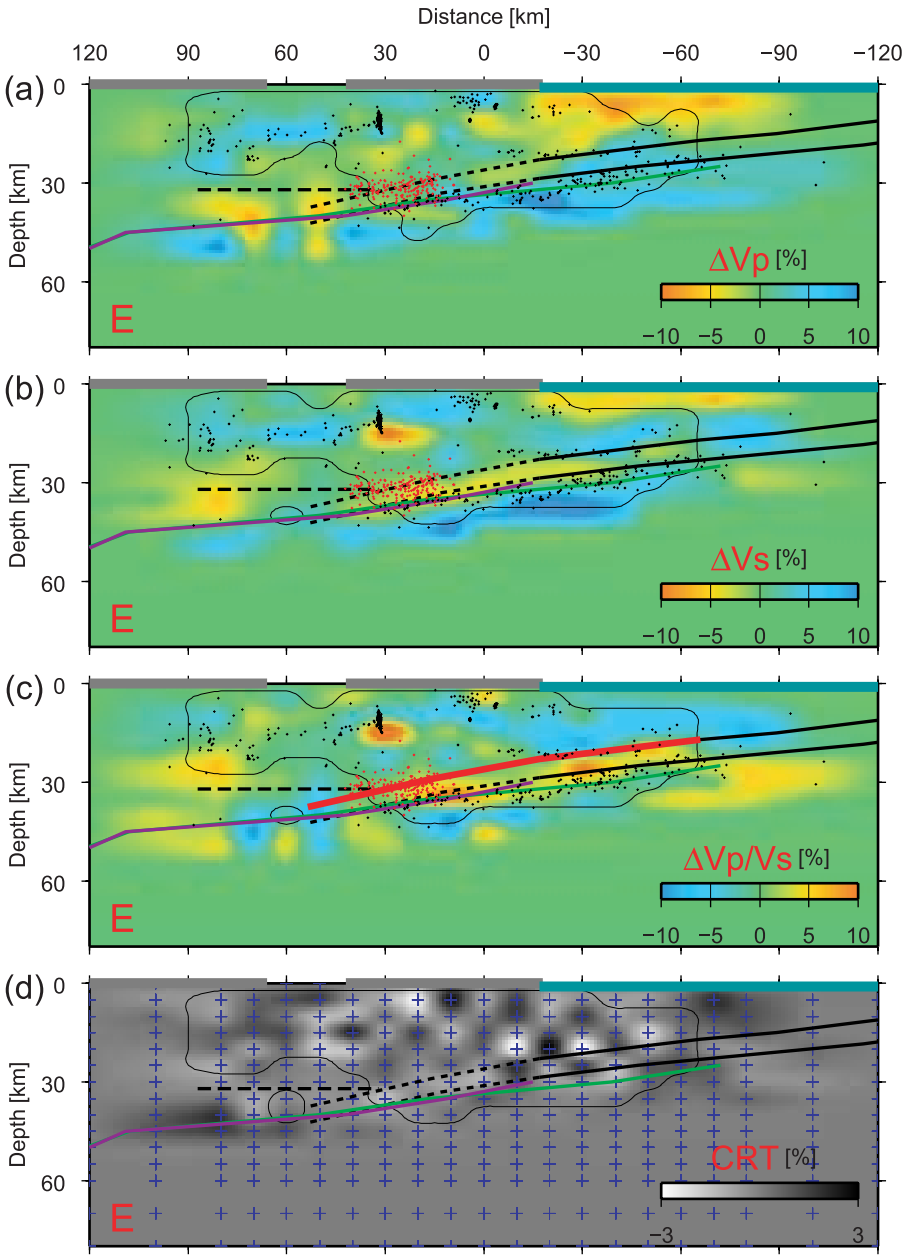

Figure 12. Vertical cross sections of (a) P wave and (b) S wave velocity perturbations, (c) Vp/Vs ratio perturbations, and (d) CRTs for S wave velocity along line E in Figure 2. Solid black lines denote the plate boundary and the slab Moho estimated by seismic reflection and refraction survey [*Kodaira et al.*, 2000], and dashed lines denote the island arc Moho [*Ikami et al.*, 1982; *Kodaira et al.*, 2000]. Other symbols are the same as those in Figures 5 and 9.

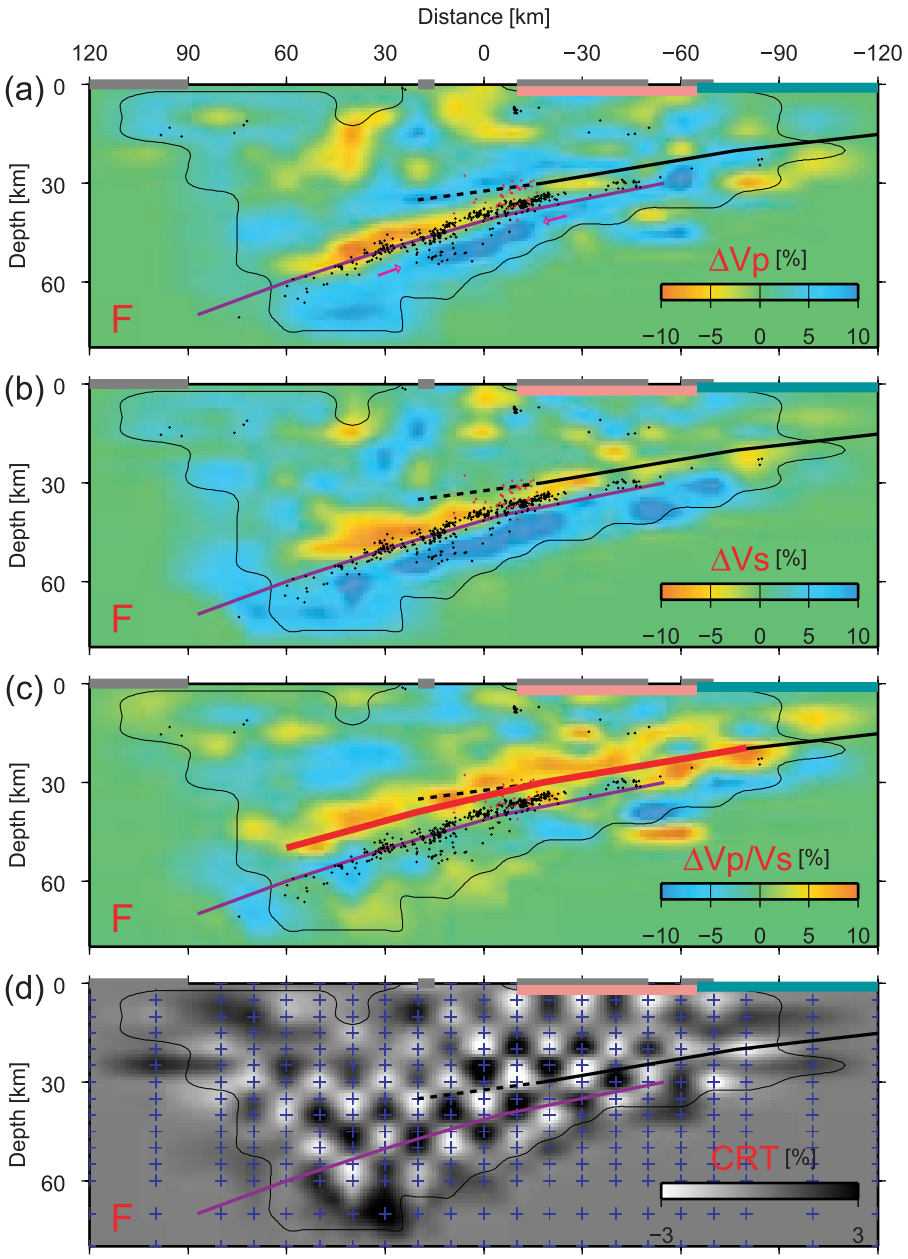

Figure 13. Vertical cross sections of (a) P wave and (b) S wave velocity perturbations, (c) Vp/Vs ratio perturbations, and (d) CRTs for S wave velocity along line F in Figure 2. Solid black lines denote the plate boundary estimated by seismic reflection and refraction survey [*Takahashi et al.*, 2002], and pink line denotes the surface locations of long-term slow slip events [*Hirose et al.*, 1999; *Ozawa et al.*, 2001]. Other symbols are the same as those in Figures 5 and 9.

intervals down to a depth of 60 km, and at 20 km intervals at greater depth in Figure 18.

[25] The present estimate is made on the basis of low-Vs and high-Vp/Vs layer, whereas *Nakajima and Hasegawa* [2007] estimated the location of the plate boundary from the distribution of high-velocity anomalies. At first glance, these approaches appear contradictory, although the results are connected smoothly in Figure 18. There are two reasons of the smooth connection of the plate boundary between two studies. One is that, since the low-Vs and high-Vp/Vs oceanic crust could release water under the high-temperature and high-pressure conditions and transform into higher-density and high-velocity minerals, the low-Vs layer would not exist at deeper depths [*Hacker et al.*, 2003]. The other is that the analysis of *Nakajima and Hasegawa* [2007] does not have sufficient resolution to detect a thin crust of just several kilometers in thickness.

[26] Figure 19 shows the comparison of the configuration of the Philippine Sea slab estimated in this study with that by *Noguchi* [1996] and *Miyoshi and Ishibashi* [2004]. *Noguchi* [1996] and *Miyoshi and Ishibashi* [2004] determined the plate boundary partly in Tokai and in Kinki and

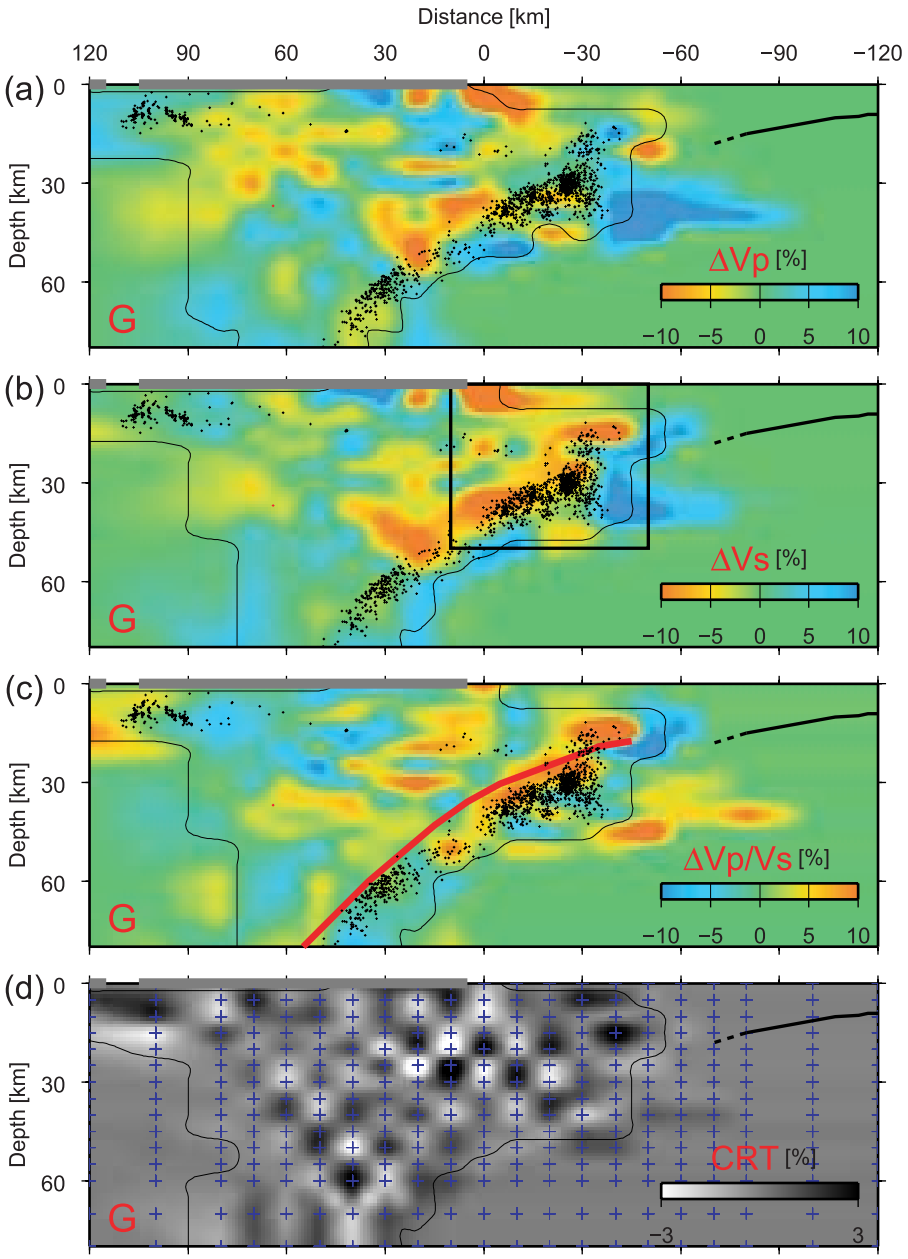

Figure 14. Vertical cross sections of (a) P wave and (b) S wave velocity perturbations, (c) Vp/Vs ratio perturbations, and (d) CRTs for S wave velocity along line G in Figure 2. Solid black lines denote the plate boundary estimated by seismic reflection and refraction survey [*Ichikawa et al.*, 1997]. Rectangle in Figure 14b shows the area magnified in Figure 17. Other symbols are the same as those in Figure 9.

Shikoku, respectively, based on the upper envelope of hypocenters. The configuration of the plate boundary is similar to each other but the depth of the plate boundary estimated in this study is generally 5–7 km shallower than their studies, since the low-Vs and high-Vp/Vs layer is additionally taken into consideration in this study.

5. Discussion

5.1. Seismic Activity in the Philippine Sea Slab

[27] Beneath Tokai, the Kii Peninsula and Shikoku, a distinct pair of later P and S phases is frequently observed after initial P and S phases for earthquakes at depths less than 60 km [e.g., *Fukao et al.*, 1983; *Hori et al.*, 1985; *Oda et al.*, 1990; *Ohkura*, 2000]. The events with later phases are considered to occur in the oceanic crust. On the other hand, *Kurashimo et al.* [2002] suggested that most of intraslab earthquakes beneath eastern Shikoku (Figures 11 and 12) occur in the slab mantle. A comparison of the upper interface of the Philippine Sea slab with the distribution of intraslab earthquakes estimated in this study (Figures 5–7 and 9–14) suggests that most of the intraslab earthquakes do not occur at least in the upper part of the oceanic

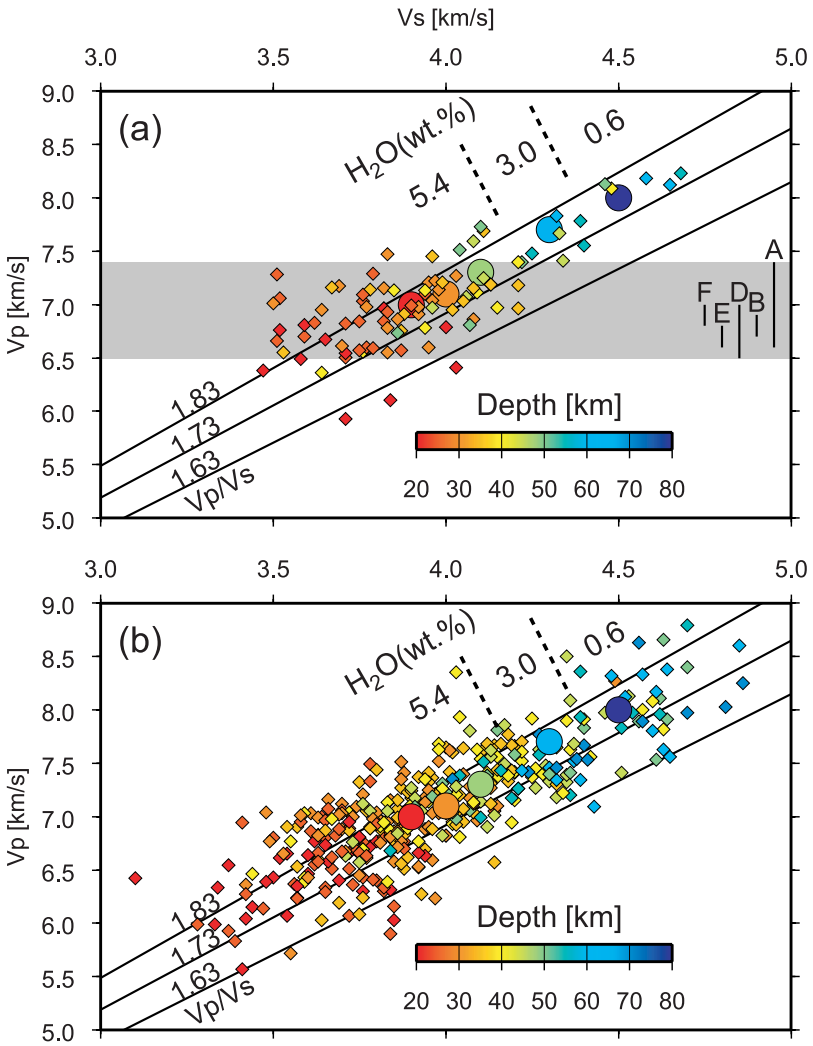

Figure 15. Vp versus Vs plot at the grid nodes located in the oceanic crust at (a) lines A–G and (b) lines 3–25 in Figure 2. Diamonds and circles represent the observations and the seismic velocities of the oceanic crust expected from phase diagram and thermal model for Nankai, SW Japan [*Hacker et al.*, 2003]. Color indicates the depth of the data points. The values of H_2O (wt %) estimated by *Hacker et al.* [2003] are also shown. A gray zone in Figure 15a denotes the range of P wave velocities (Vp = 6.5–7.4 km/s) in the oceanic crust (oceanic layer 3) estimated by the seismic reflection and refraction surveys (A, *Kodaira et al.* [2004]; B, *Nakanishi et al.* [2002]; D, *Kodaira et al.* [2002]; E, *Kodaira et al.* [2000]; F, *Takahashi et al.* [2002]) at depths of 20–40 km.

crust but rather occur in the lower part of the oceanic crust and the slab mantle.

[28] It has been argued that the double seismic zone is formed within the Philippine Sea slab, in particular beneath the Kii Peninsula [e.g., *Seno et al.*, 2001]. *Yamaoka and Nishihara* [1997] and *Miyoshi and Ishibashi* [2004] argued that the double seismic zone within the slab beneath the Kii Peninsula may be apparent due to splitting of the slab into two in the vicinity of the Ise Bay to the Kii Peninsula, where the eastern slab slides over the western slab. However, *Miyoshi and Ishibashi* [2004] also suggested that the possibility of a double seismic zone in a continuous slab cannot be ruled out. From the detailed hypocenter distribution obtained in this study, the lower seismic plane of the double seismic zone can be traced all the way from the Ise Bay to southern Kyushu (lines 4 to 24 in Figure 5, lines B to D, and F in Figures 9–11, and 13), although the seismic activity varies from one region to another. This implies that the double seismic zone is actually formed even in the Philippine Sea slab, similarly to the case of the Pacific slab [*Umino and Hasegawa*, 1975; *Hasegawa et al.*, 1978].

5.2. High-Vp/Vs Anomaly Around Source Regions of Long-Term Slow Slip Event

[29] Beneath the Bungo Channel, long-term slow slip events had occurred for a period of about 1 year from the end of 1996, and then again for about half a year from August 2003 [*Hirose et al.*, 1999; *Ozawa et al.*, 2001; *Geographical Survey Institute*, 2004]. The projections of those events to the ground surface are shown as pink solid

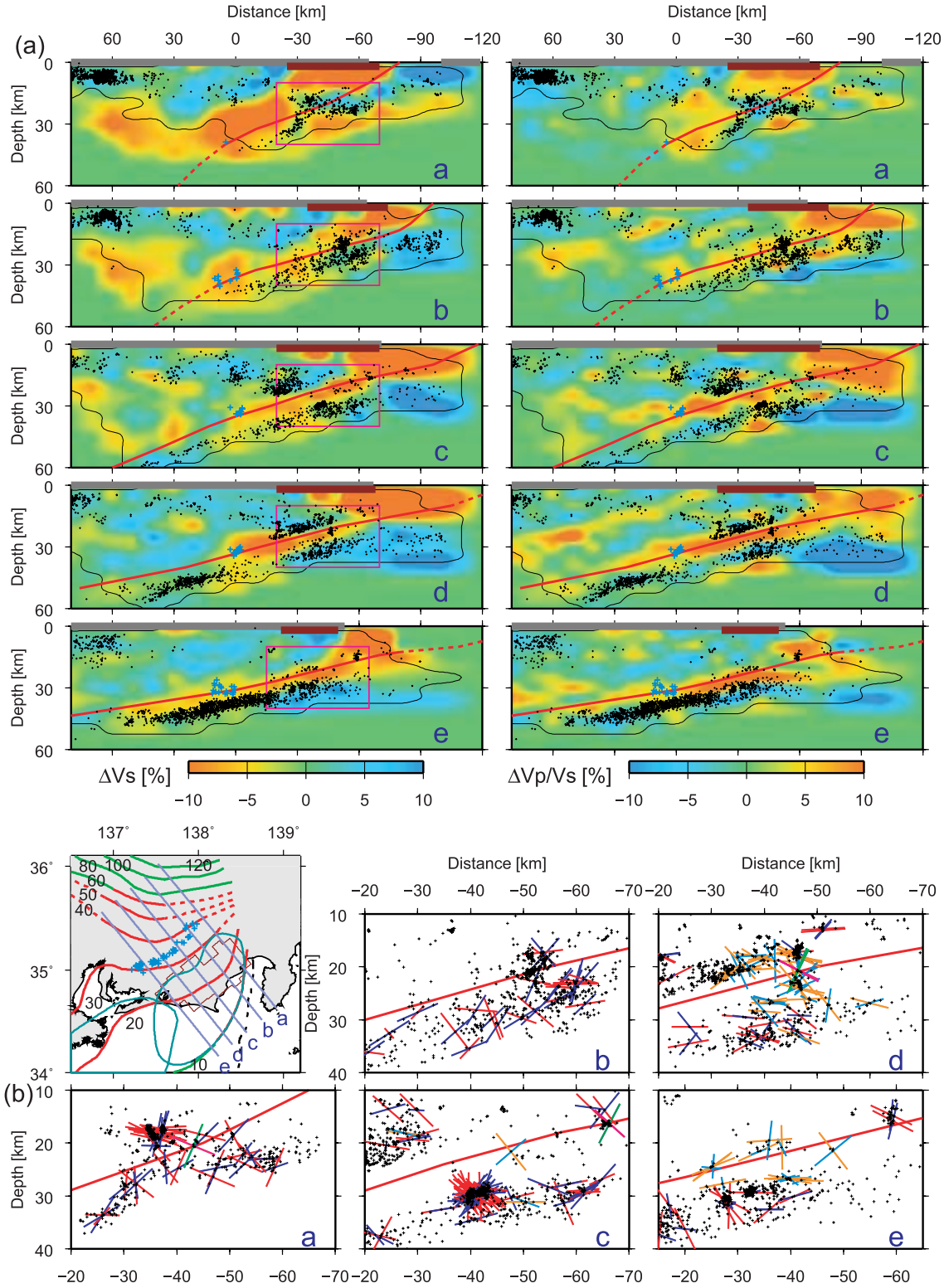

Figure 16. (a) Vertical cross sections of perturbations of S wave velocity and Vp/Vs ratio and (b) distribution of P axis (red or orange or purple) and T axis (blue or light blue or green) of focal mechanisms derived from first motion data for the purple rectangles in plots of Vs, along lines a to e in the inset map. Red lines show estimated location of plate boundary. P and T axes of focal mechanisms newly determined in this study are indicted by orange and light blue lines, while those determined by the JMA are shown by red and blue lines. Note that four events near plate boundary which have low-angle and thrust-type focal mechanism solutions are shown by purple (P axis) and green (T axis) lines (a, M2.0 on 18 July 2005; c, M2.8 on 28 July 2001; d, M1.5 on 24 November 2002; and M2.1 on 25 November 2002). Other symbols are the same as those in Figures 5 and 7.

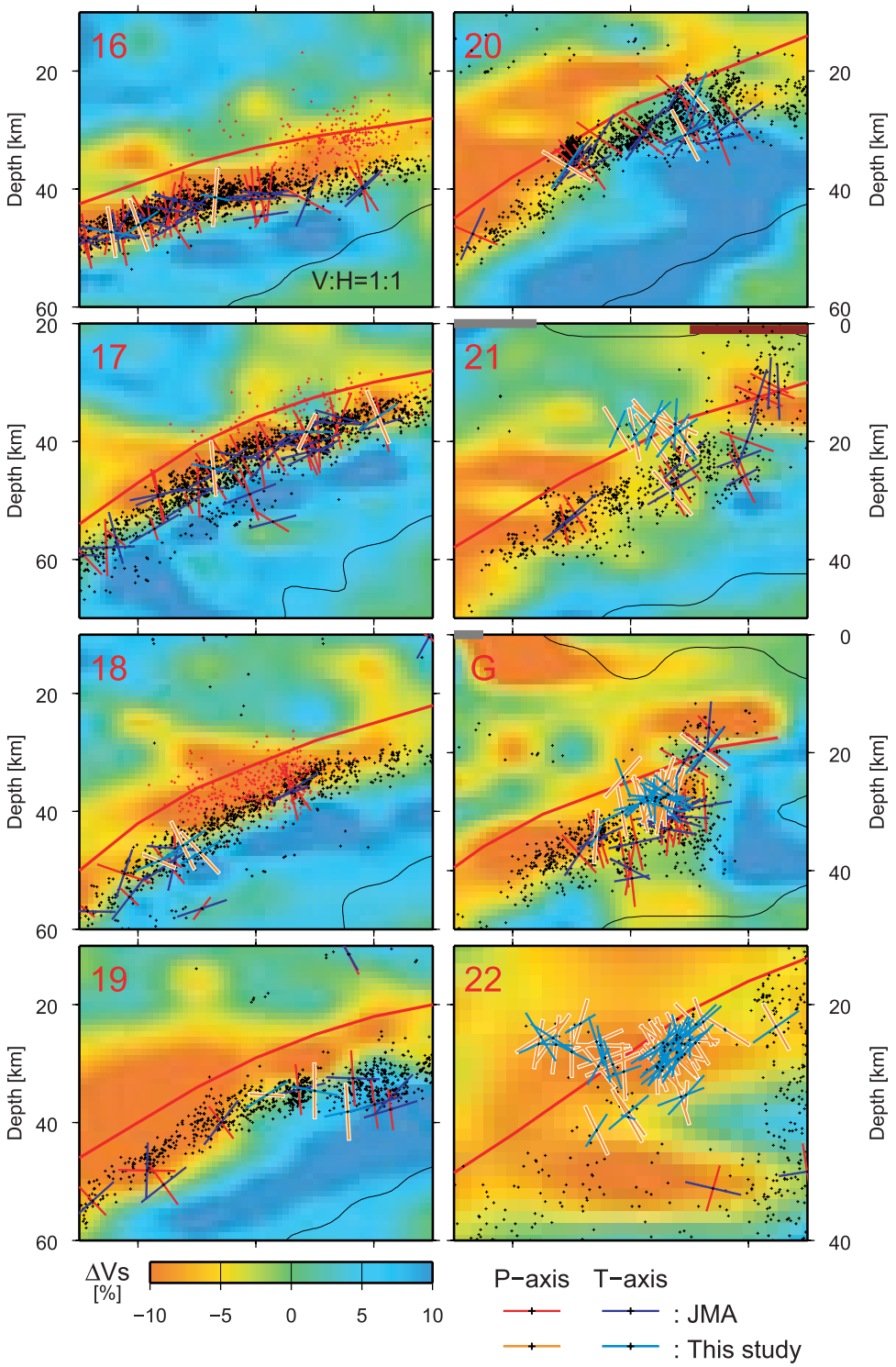

Figure 17. Vertical cross sections of perturbations of S wave velocity together with distribution of P axis (red or orange) and T axis (blue or light blue) of focal mechanisms derived from first motion data for the rectangles in plots of lines 16–22 in Figure 5 and Figure 14b. P and T axes of focal mechanisms newly determined in this study are indicted by orange and light blue lines, while those determined by the JMA are shown by red and blue lines. Other symbols are the same as those in Figure 5.

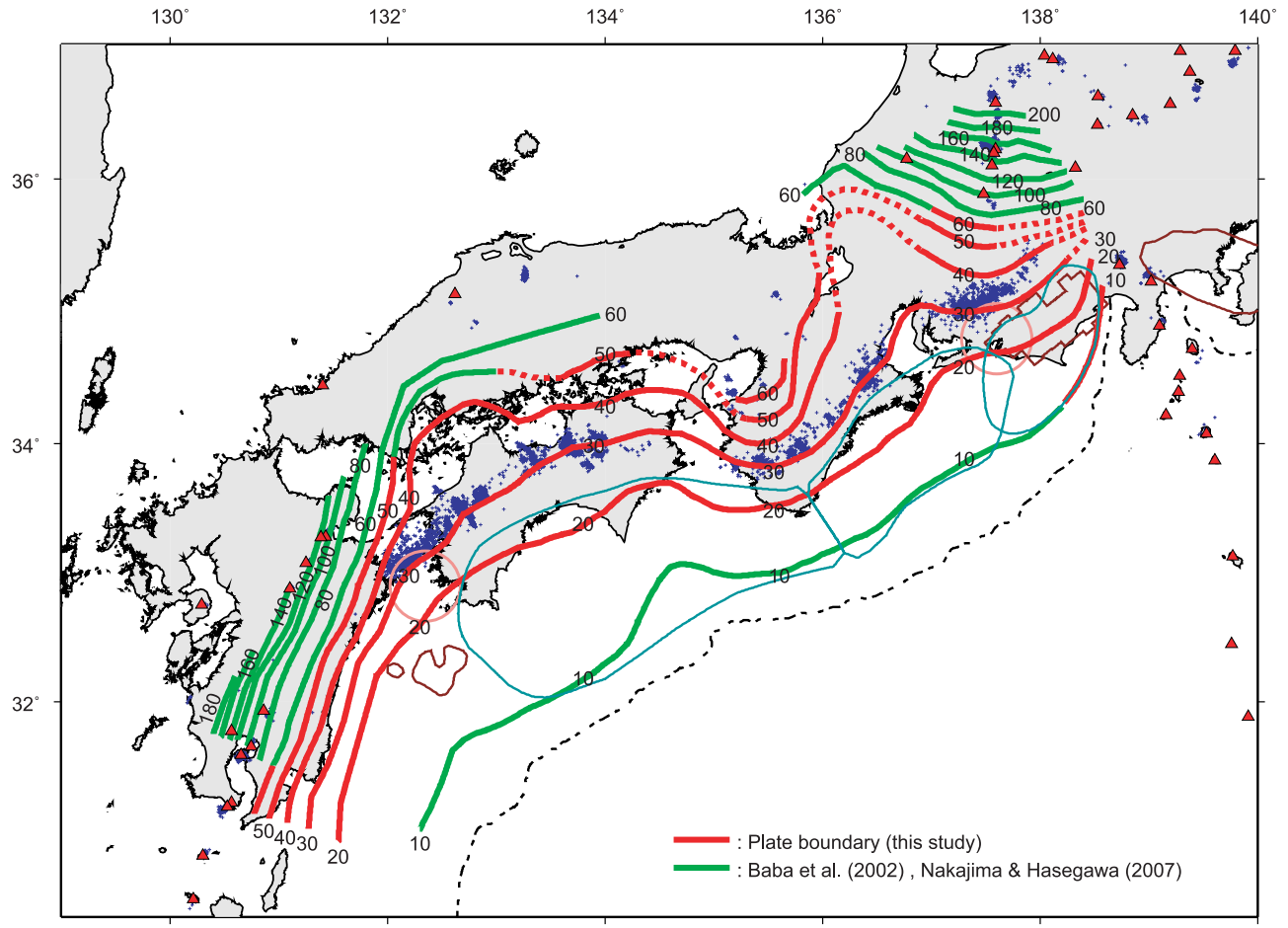

Figure 18. Depth contour map of the upper boundary of the Philippine Sea slab (10 and 20 km intervals). The isodepth contour of 10 km is taken from *Baba et al.* [2002], who estimated the upper boundary of the Philippine Sea slab from offshore reflection and refraction surveys, while the isodepth contours of 60–200 km are taken from *Nakajima and Hasegawa* [2007], who estimated the upper boundary of the Philippine Sea slab from seismic tomography. Blue crosses denote deep low-frequency earthquakes. Note that deep low-frequency earthquakes associated with volcanic activity are also shown. Other symbols are the same as those in Figure 1.

lines in Figure 13. When hydrated minerals in the oceanic crust subducting to great depth undergo a phase transformation, a large amount of water is liberated [e.g., *Hacker et al.*, 2003]. Consequently, pore pressure on the plate boundary increases accompanied by dehydration reactions, which in turn decreases effective normal stress and weakens coupling on the plate boundary. *Liu and Rice* [2005] simulated that intermittent slow sliding occurs in weak coupling transition area between locked area at shallower region and steady sliding area at deeper region. Therefore, the existence of water due to dehydration from the slab might cause long-term slow slip events. A prominent high-Vp/Vs region immediately above the presumed plate boundary beneath Bungo Channel (Figure 13) may correspond to a hydrous layer that contains serpentine and/or chlorite resulting from reaction of peridotite with water supplied from the Philippine Sea slab [e.g., *Tatsumi*, 1989; *Iwamori*, 1998; *Kawakatsu and Watada*, 2007]. The occurrence of long-term slow slips events as well as serpentinized mantle wedge is attributable to the release of a relatively large amount of water by dehydration reactions in the subducting slab.

[30] The long-term slow slips event is also observed in Tokai region (line 3 in Figure 6 and line A in Figure 7) [*Ozawa et al.*, 2002; *Miyazaki et al.*, 2006]. The fact that a high-Vp/Vs layer is distributed at the mantle wedge again implies that the water released from the slab might trigger the long-term slow slip event by increasing pore pressure along the plate boundary and consequently migrate upward into the mantle wedge, causing a high-Vp/Vs anomaly there.

5.3. Depth Distribution of Deep Low-Frequency Earthquakes and Implications for Their Occurrences

[31] Figure 18 shows that nonvolcanic deep low-frequency earthquakes are distributed in a belt-like form along the isodepth contour of 30 km depth of the plate boundary estimated in this study, as pointed out by *Obara* [2002]. However, it appears that at northeastern Tokai district deep low-frequency earthquakes are distributed away from the

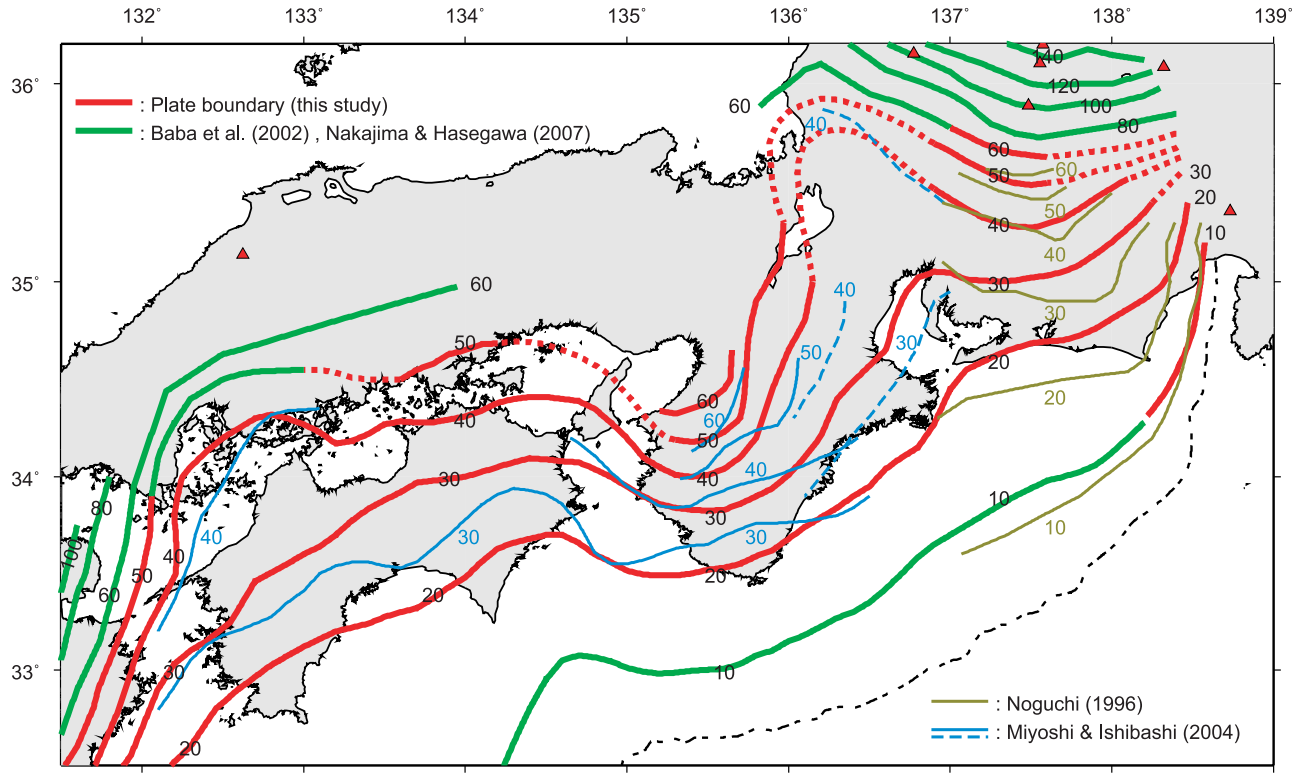

Figure 19. Comparison of the configurations of the Philippine Sea slab. Gold and blue lines denote the plate configuration estimated by *Noguchi* [1996] and *Miyoshi and Ishibashi* [2004], respectively. Other symbols are the same as those in Figure 18.

isodepth contour of 30 km depth of the plate boundary and lie on the isodepth contour of 40 km depth. *Ide et al.* [2007] analyzed mechanism of deep low-frequency earthquakes and suggested that deep low-frequency earthquakes are generated by shear slip on the plate interface. If they occur on the plate boundary even at the Tokai district, it is expected that their depths become deeper at northeastern Tokai.

[32] It is known that deep low-frequency earthquakes occur during continuous deep low-frequency tremors [*Shelly et al.*, 2007] and tend to occur in succession in the Tokai district [*Kobayashi et al.*, 2006], which makes it difficult to pick P and/or S phases accurately. As a result, the depth distribution of deep low-frequency earthquakes is scattered in depth ranges of 20–50 km as shown in Figure 20a. To constrain and precisely estimate the depth of deep low-frequency earthquakes, we selected 69 deep low-frequency earthquakes (red circles in Figure 20a) from 1582 events in the JMA catalog (gray circles in Figure 20a) that occurred from 1 November 2002 to 31 December 2006 at the Tokai district. The selection is based on the following criteria: (1) P wave arrival times are picked at more than three stations, (2) total number of P and S wave arrival times picked are 10 or more, and (3) the magnitude is greater than 0.0. We checked waveforms of the 69 events and repicked P and S wave arrival times. In the picking procedure, we noticed several wrong phase pickings resulting from the continuous occurrence of low-frequency earthquakes. Some of the events with wrong phase pickings were determined at a depth of 45 km in the JMA catalog with traveltime residuals of more than 1 s. We excluded those wrong pickings and unclear phases and picked only clear phases in each seismogram, which yields 53 deep low-frequency earthquakes recorded by 10 or more stations. Then, the 53 events were relocated with one-dimensional JMA2001 seismic velocity model [*Ueno et al.*, 2002]. After that, they were relocated with the three-dimensional velocity structure estimated in this study, by applying DD location algorithm [*Waldhauser and Ellsworth*, 2000], together with regular earthquakes that occur within the slab and in the overriding plate. As a result, deep low-frequency earthquakes were clustered and located at a depth of ~30 km in the southwestern part and at depths of 35–40 km in the northeastern part, indicating a gradual deepening of deep low-frequency earthquakes from southwest to northeast (Figure 20b).

[33] The existence of water supplied by dehydration reaction is believed to cause deep low-frequency earthquakes and tremors by increasing pore pressure on the plate boundary [*Obara*, 2002]. Such deep low-frequency earthquakes do not occur in the Ise Bay and the Kii Channel. Looking at the S wave velocity structure along line 5 across the Ise Bay (Figure 5) and the Vp/Vs ratio (Figure 6), the low-Vs and high-Vp/Vs layer immediately above the intraslab earthquakes is not as clear as in other regions. This observation suggests that the intensive dehydration reaction itself might not occur in this vicinity.

[34] Along line 10, which crosses the Kii Channel, the high-Vp/Vs layer immediately above the intraslab earthquakes is distinct, hinting at the presence of fluids. This implies that the occurrence of deep low-frequency earthquakes is dependent not only on the presence of fluids but

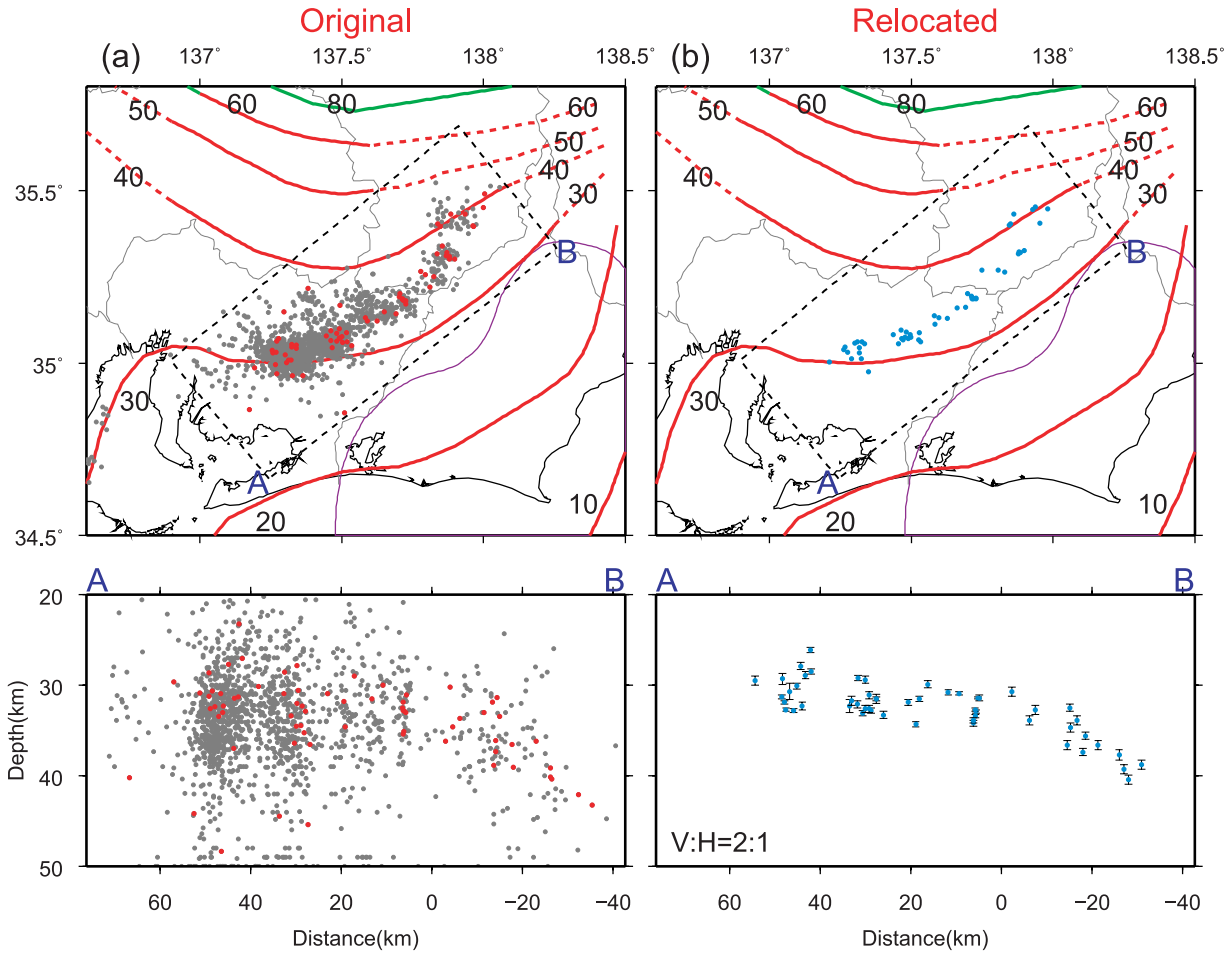

Figure 20. Distribution of nonvolcanic deep low-frequency earthquakes. (a) Original hypocenters in the JMA catalog. Gray circles denote 1582 events that occurred from 1 November 2002 to 31 December 2006 at the Tokai district. Red circles denote 69 events ($M \geq 0.0$) that have 3 or more P wave pickings and are recorded by 10 or more stations. (b) Hypocenters relocated in this study. Blue circles denote 53 events recorded by 10 or more stations, which were relocated with the three-dimensional velocity structure estimated in this study, by applying double-difference location algorithm [*Waldhauser and Ellsworth*, 2000]. Relocation errors in depth are shown by bars. See text for further details.

also on other factors. Isodepth contours of the Philippine Sea slab in regions where deep low-frequency earthquakes do not occur are curved, indicating that the shape of the plate changes suddenly. Furthermore, in the Kii Channel, the direction of relative plate motion is parallel to the isodepth contours. These factors could be partly responsible for the absence of deep low-frequency earthquakes. Long-term slow slip events that occur in Lake Hamana in the Tokai region and in the Bungo Channel [*Hirose et al.*, 1999; *Ozawa et al.*, 2001, 2002; *Miyazaki et al.*, 2006] are located at depths of 20–30 km, adjacent to the shallow part of the region characterized by particularly elevated activity of deep low-frequency earthquakes.

6. Conclusions

[35] With the aim of deepening our understanding of seismotectonics and specifically the structure of the Philippine Sea plate subducting beneath SW Japan, the double-difference tomography was employed to estimate the three-dimensional seismic velocity structure in the crust and upper mantle in the regions from Tokai to southern Kyushu. The principal results are as follows.

[36] 1. It has become clear that in most of the region from Tokai to southern Kyushu, there exists a low-Vs and high-Vp/Vs layer of several kilometers in thickness immediately above the region of intraslab earthquake activity.

[37] 2. Comparison with the results of seismic reflection and refraction surveys suggests that the low-Vs and high-Vp/Vs layer, which is inclined in the direction of plate subduction, corresponds to the oceanic crust. The upper limit of this low-Vs and high-Vp/Vs layer is interpreted to be the plate boundary and a new configuration of the Philippine Sea slab is proposed in the regions from Tokai to Kyushu.

[38] 3. Deep low-frequency earthquakes are distributed along the isodepth contours of 30 km depth of the Philippine Sea slab from Kinki to the Bungo Channel. However, the

depth of deep low-frequency earthquakes becomes gradually deeper from southwest to northeast in the Tokai district and reaches to a depth of $\sim$ 40 km in the northeastern part.

[39] **Acknowledgments.** We would like to thank H. Zhang and C. H. Thurber for providing us with the tomoFDD program. This manuscript was greatly improved by careful reviews of G. Lin, an anonymous reviewer, and J. Revenaugh, an Associate Editor. We used seismic data from the National Research Institute for Earth Science and Disaster Prevention, Hokkaido University, Hirosaki University, Tohoku University, University of Tokyo, Nagoya University, Kyoto University, Kochi University, Kyushu University, Kagoshima University, the Japan Meteorological Agency, the National Institute of Advanced Industrial Science and Technology, the Geographical Survey Institute, Aomori prefectural government, Tokyo metropolitan government, Shizuoka prefectural government, Kanagawa prefectural government, the City of Yokohama, and the Japan Marine Science and Technology Center. Figures were prepared using GMT [*Wessel and Smith*, 1991].

References

Baba, T., Y. Tanioka, P. R. Cummins, and K. Uhira (2002), The slip distribution of the 1946 Nankai earthquake estimated from tsunami inversion using a new plate model, *Phys. Earth Planet. Inter.*, *132*, 59–73, doi:10.1016/S0031-9201(02)00044-4.

Fukao, Y., S. Hori, and M. Ukawa (1983), A seismological constraint on the depth of basalt-eclogite transition in a subducting oceanic crust, *Nature*, *303*, 413–415, doi:10.1038/303413a0.

Geographical Survey Institute (2004), Crustal movements in the Chugoku, Shikoku and Kyushu districts (in Japanese), *Rep. Coord. Comm. Earthquake Predict.*, *71*, 680–694.

Grand, S. P. (1987), Tomographic inversion for shear velocity beneath the North American plate, *J. Geophys. Res.*, *92*(B13), 14,065–14,090, doi:10.1029/JB092iB13p14065.

Hacker, B. R., G. A. Abers, and S. M. Peacock (2003), Subduction factory: 1. Theoretical mineralogy, densities, seismic wave speeds, and H_2O contents, *J. Geophys. Res.*, *108*(B1), 2029, doi:10.1029/2001JB001127.

Hasegawa, A., N. Umino, and A. Takagi (1978), Double-planed structure of the deep seismic zone in the northeastern Japan arc, *Tectonophysics*, *47*, 43–58, doi:10.1016/0040-1951(78)90150-6.

Heki, K., and S. Miyazaki (2001), Plate convergence and long-term crustal deformation in central Japan, *Geophys. Res. Lett.*, *28*, 2313–2316, doi:10.1029/2000GL012537.

Hirose, H., K. Hirahara, F. Kimata, N. Fujii, and S. Miyazaki (1999), A slow thrust slip event following the two 1996 Hyuganada earthquakes beneath the Bungo Channel, southwest Japan, *Geophys. Res. Lett.*, *26*, 3237–3240, doi:10.1029/1999GL010999.

Honda, S., and I. Nakanishi (2003), Seismic tomography of the uppermost mantle beneath southwestern Japan: Seismological constraints on modeling subduction and magmatism for the Philippine Sea slab, *Earth Planets Space*, *55*, 443–462.

Hori, S., H. Inoue, Y. Fukao, and M. Ukawa (1985), Seismic detection of the untransformed 'basaltic' oceanic crust subducting into the mantle, *Geophys. J.R. Astron. Soc.*, *83*, 169–197.

Ichikawa, G., T. Shirogane, A. Nakanishi, H. Shiobara, H. Shimamura, R. Hino, T. Yamada, H. Sugioka, and T. Kanazawa (1997), Ocean bottom seismographic experiment to study crustal structure in Hyuganada, paper presented at Japanese Earth and Planetary Sciences Joint Meeting, Geod. Soc. of Jpn., Aichi, Japan.

Ide, S., D. R. Shelly, and G. C. Beroza (2007), Mechanism of deep low frequency earthquakes: Further evidence that deep non-volcanic tremor is generated by shear slip on the plate interface, *Geophys. Res. Lett.*, *34*, L03308, doi:10.1029/2006GL028890.

Ikami, A., K. Ito, Y. Sasaki, and S. Asano (1982), Crustal structure in the profile across Shikoku, Japan as derived from the off Sakaide explosions in March, 1975 (in Japanese with English abstract), *J. Seismol. Soc. Jpn.*, *2*(35), 367–375.

Ishida, M. (1992), Geometry and relative motion of the Philippine Sea plate and Pacific plate beneath the Kanto-Tokai district, Japan, *J. Geophys. Res.*, *97*(B1), 489–513, doi:10.1029/91JB02567.

Ito, K., et al. (2005), Seismic reflectors and subduction of Philippine Sea plate from the seismic survey along the Shingu-Maizuru line, in the Kinki district, Japan, paper presented at 2005 Fall Meeting, Seismol. Soc. Jpn., Sapporo, Japan.

Ito, Y., K. Obara, K. Shiomi, S. Sekine, and H. Hirose (2007), Slow earthquakes coincident with episodic tremors and slow slip events, *Science*, *315*, 503–506, doi:10.1126/science.1134454.

Iwamori, H. (1998), Transportation of H2O and melting in subduction zones, *Earth Planet. Sci. Lett.*, *160*, 65–80, doi:10.1016/S0012-821X(98)00080-6.

Kawakatsu, H., and S. Watada (2007), Seismic evidence for deep-water transportation in the Mantle, *Science*, *316*, 1468–1471, doi:10.1126/science.1140855.

Kobayashi, A., T. Yamamoto, K. Nakamura, and K. Kimura (2006), Short-term slow slip events detected by the strainmeters in Tokai region in the period from 1984 to 2005 (in Japanese with English abstract), *J. Seismol. Soc. Jpn.*, *2*(59), 19–27.

Kodaira, S., N. Takahashi, J. Park, K. Mochizuki, M. Shinohara, and S. Kimura (2000), Western Nankai Trough seismogenic zone: Results from a wide-angle ocean bottom seismic survey, *J. Geophys. Res.*, *105*(B3), 5887–5905, doi:10.1029/1999JB900394.

Kodaira, S., E. Kurashimo, J. Park, N. Takahashi, A. Nakanishi, S. Miura, T. Iwasaki, N. Hirata, K. Ito, and Y. Kaneda (2002), Structural factors controlling the rupture process of a megathrust earthquake at the Nankai trough seismogenic zone, *Geophys. J. Int.*, *149*, 815–835, doi:10.1046/j.1365-246X.2002.01691.x.

Kodaira, S., T. Iidake, A. Kato, J. Park, T. Iwasaki, and Y. Kaneda (2004), High pore fluid pressure may cause silent slip in the Nankai Trough, *Science*, *304*, 1295–1298, doi:10.1126/science.1096535.

Kurashimo, E., M. Tokunaga, N. Hirata, T. Iwasaki, S. Kodaira, Y. Kaneda, K. Ito, R. Nishida, S. Kimura, and T. Ikawa (2002), Geometry of the subducting Philippine Sea plate and the crustal and upper mantle structure beneath eastern Shikoku island revealed by seismic refraction/wide-angle reflection profiling (in Japanese with English abstract), *J. Seismol. Soc. Jpn.*, *2*(54), 489–505.

Liu, Y., and J. R. Rice (2005), Aseismic slip transients emerge spontaneously in three-dimensional rate and state modeling of subduction earthquake sequences, *J. Geophys. Res.*, *110*, B08307, doi:10.1029/2004JB003424.

Matsumura, S. (1997), Focal zone of a future Tokai earthquake inferred from the seismicity pattern around the plate interface, *Tectonophysics*, *273*, 271–291, doi:10.1016/S0040-1951(96)00277-6.

Miyazaki, S., and K. Heki (2001), Crustal velocity field of southwest Japan: Subduction and arc-arc collision, *J. Geophys. Res.*, *106*(B3), 4305–4326, doi:10.1029/2000JB900312.

Miyazaki, S., P. Segall, J. J. McGuire, T. Kato, and Y. Hatanaka (2006), Spatial and temporal evolution of stress and slip rate during the 2000 Tokai slow earthquake, *J. Geophys. Res.*, *111*, B03409, doi:10.1029/2004JB003426.

Miyoshi, T., and K. Ishibashi (2004), Geometry of the seismic Philippine Sea slab beneath the region from Ise bay to western Shikoku, southwest Japan (in Japanese with English abstract), *J. Seismol. Soc. Jpn.*, *2*(57), 139–152.

Nakajima, J., and A. Hasegawa (2007), Subduction of the Philippine Sea plate beneath southwestern Japan: Slab geometry and its relationship to arc magmatism, *J. Geophys. Res.*, *112*, B08306, doi:10.1029/2006JB004770.

Nakanishi, A., N. Takahashi, J. O. Park, S. Miura, S. Kodaira, Y. Kaneda, N. Hirata, T. Iwasaki, and M. Nakamura (2002), Crustal structure across the coseismic rupture zone of the 1944 Tonankai earthquake, the central Nankai Trough seismogenic zone, *J. Geophys. Res.*, *107*(B1), 2007, doi:10.1029/2001JB000424.

Noguchi, S. (1996), Geometry of the Philippine Sea slab and the convergent tectonics in the Tokai district, Japan (in Japanese with English abstract), *J. Seismol. Soc. Jpn.*, *2*(49), 295–325.

Obara, K. (2002), Nonvolcanic deep tremor associated with subduction in southwest Japan, *Science*, *296*, 1679–1681, doi:10.1126/science.1070378.

Obara, K., H. Hirose, F. Yamamizu, and K. Kasahara (2004), Episodic slow slip events accompanied by non-volcanic tremors in southwest Japan subduction zone, *Geophys. Res. Lett.*, *31*, L23602, doi:10.1029/2004GL020848.

Oda, H., T. Tanaka, and K. Seya (1990), Subducting oceanic crust on the Philippine Sea plate in Southwest Japan, *Tectonophysics*, *172*, 175–189, doi:10.1016/0040-1951(90)90068-J.

Ohkura, T. (2000), Structure of the upper part of the Philippine Sea plate estimated by later phases of upper mantle earthquakes in and around Shikoku, Japan, *Tectonophysics*, *321*, 17–36, doi:10.1016/S0040-1951(00)00078-0.

Ozawa, S., M. Murakami, and T. Tada (2001), Time-dependent inversion study of the slow thrust event in the Nankai trough subduction zone, southwestern Japan, *J. Geophys. Res.*, *106*(B1), 787–802, doi:10.1029/2000JB900317.

Ozawa, S., M. Murakami, M. Kaidzu, T. Tada, T. Sagiya, Y. Hatanaka, H. Yarai, and T. Nishimura (2002), Detection and monitoring of ongoing aseismic slip in the Tokai region, central Japan, *Science*, *298*, 1009–1012, doi:10.1126/science.1076780.

Seno, T., S. Stein, and A. E. Gripp (1993), A model for the motion of the Philippine Sea plate consistent with NUVEL-1 and geological data, *J. Geophys. Res.*, *98*(B10), 17,941–17,948, doi:10.1029/93JB00782.

Seno, T., D. Zhao, Y. Kobayashi, and M. Nakamura (2001), Dehydration of serpentinized slab mantle: Seismic evidence from southwest Japan, *Earth Planets Space*, *53*, 861–871.

Shelly, D. R., G. C. Beroza, S. Ide, and S. Nakamura (2006), Low-frequency earthquakes in Shikoku, Japan, and their relationship to episodic tremor and slip, *Nature*, *442*, 188–191, doi:10.1038/nature04931.

Shelly, D. R., G. C. Beroza, and S. Ide (2007), Non-volcanic tremor and low-frequency earthquake swarms, *Nature*, *446*, 305–307, doi:10.1038/nature05666.

Shiomi, K., M. Matsubara, and K. Obara (2006), Configuration of Philippine Sea plate beneath the central and western part of Japan from teleseismic receiver function analysis, paper presented at 6th Joint Meeting of UJNR Panel on Earthquake Research, UJNR Panel on Earthquake Res. Tokushima, Japan.

Takahashi, N., et al. (2002), Seismic structure of western end of the Nankai trough seismogenic zone, *J. Geophys. Res.*, *107*(B10), 2212, doi:10.1029/2000JB000121.

Tatsumi, Y. (1989), Migration of fluid phases and genesis of basalt magmas in subduction zones, *J. Geophys. Res.*, *94*(B4), 4697–4707, doi:10.1029/JB094iB04p04697.

Thurber, C., and D. Eberhart-Phillips (1999), Local earthquake tomography with flexible gridding, *Comput. Geosci.*, *25*, 809–818, doi:10.1016/S0098-3004(99)00007-2.

Ueno, H., S. Hatakeyama, T. Aketagawa, J. Funasaki, and N. Hamada (2002), Improvement of hypocenter determination procedures in the Japan Meteorological Agency (in Japanese with English abstract), *Q. J. Seismol.*, *65*, 123–134.

Umino, N., and A. Hasegawa (1975), On the two-layered structure of deep seismic plane in northeastern Japan arc (in Japanese with English abstract), *J. Seismol. Soc. Jpn.*, *27*, 125–139.

Wald, D. J., and P. G. Somerville (1995), Variable-slip rupture model of the great 1923 Kanto, Japan, earthquake: Geodetic and body-waveform analysis, *Bull. Seismol. Soc. Am.*, *85*, 159–177.

Waldhauser, F., and W. L. Ellsworth (2000), A double-difference earthquake location algorithm: Method and application to the northern Hayward fault, California, *Bull. Seismol. Soc. Am.*, *90*, 1353–1368, doi:10.1785/0120000006.

Wang, Z., and D. Zhao (2006), Vp and Vs tomography of Kyushu, Japan: New insight into arc magmatism and forearc seismotectonics, *Phys. Earth Planet. Inter.*, *157*, 269–285, doi:10.1016/j.pepi.2006.04.008.

Wang, K., I. Wada, and Y. Ishikawa (2004), Stresses in the subducting slab beneath southwest Japan and relation with plate geometry, tectonic forces, slab dehydration, and damaging earthquakes, *J. Geophys. Res.*, *109*, B08304, doi:10.1029/2003JB002888.

Wei, D., and T. Seno (1998), Determination of the Amurian plate motion, in *Mantle dynamics and plate interactions in East Asia*, *Geodyn. Ser.*, vol. 27, edited by M. F. J. Flower et al., pp. 337–346, AGU, Washington, D. C.

Wessel, P., and W. H. F. Smith (1991), Free software helps map and display data, *Eos Trans. AGU*, *72*, 441, doi:10.1029/90EO00319.

Yagi, Y., M. Kikuchi, S. Yoshida, and Y. Yamanaka (1998), Source process of the Hyuga-nada earthquake of April 1, 1968 (MJMA7.5), and its relationship to the subsequent seismicity (in Japanese with English abstract), *J. Seismol. Soc. Jpn.*, *2*(51), 139–148.

Yamaoka, K., and M. Nishihara (1997), Geometry of subducting Philippine Sea plate and its relationship with the volcanism in Chubu district, Japan (in Japanese with English abstract), *Bull. Volcanol. Soc. Jpn.*, *42*, S131–S138.

Yamauchi, M., K. Hirahara, and T. Shibutani (2003), High resolution receiver function imaging of the seismic velocity discontinuities in the crust and the uppermost mantle beneath southwest Japan, *Earth Planets Space*, *55*, 59–64.

Zhang, H., and C. H. Thurber (2003), Double-Difference Tomography: The method and its application to the Hayward Fault, California, *Bull. Seismol. Soc. Am.*, *93*, 1875–1889, doi:10.1785/0120020190.

Zhang, H., and C. Thurber (2006), Development and applications of double-difference seismic tomography, *Pure Appl. Geophys.*, *163*, 373–403, doi:10.1007/s00024-005-0021-y.

Zhao, D., A. Hasegawa, and S. Horiuchi (1992), Tomographic imaging of P and S wave velocity structure beneath northeastern Japan, *J. Geophys. Res.*, *97*(B13), 19,909–19,928, doi:10.1029/92JB00603.

A. Hasegawa and J. Nakajima, Research Center for Prediction of Earthquakes and Volcanic Eruptions, Graduate School of Science, Tohoku University, Aramaki-aza-Aoba, Aoba-ku, Sendai 980-8578, Japan.

F. Hirose, Seismology and Volcanology Research Department, Meteorological Research Institute, Nagamine 1-1, Tsukuba 305-0052, Japan. (fhirose@mri-jma.go.jp)